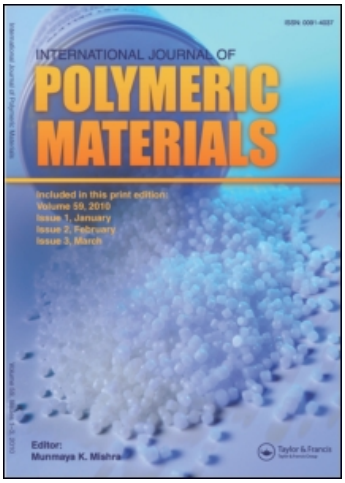

International Journal of Polymeric Materials
Publication details, including instructions for authors and subscription information:
http://www.informaworld.com/smpp/title~content=t713647664

Optical Properties of Polymer-dispersed Liquid Crystals

Francesco Simoni[a]; Oriano Francescangeli[a]
[a] Dipartimento di Scienze dei Materiali e della Tierra, Universita diAncona, Ancona, Italy

To cite this Article Simoni, Francesco and Francescangeli, Oriano(2000) 'Optical Properties of Polymer-dispersed Liquid Crystals', International Journal of Polymeric Materials, 45: 3, 381 — 449
To link to this Article: DOI: 10.1080/00914030008035050
URL: http://dx.doi.org/10.1080/00914030008035050

Intern. J. Polymeric Mater., 2000, Vol. 45, pp. 381–449
Reprints available directly from the publisher
Photocopying permitted by license only

Optical Properties of Polymer-dispersed Liquid Crystals

FRANCESCO SIMONI* and ORIANO FRANCESCANGELI

Dipartimento di Scienze dei Materiali e della Tierra,
Universita di Ancona, Via Brecce Bianche, 60131 Ancona, Italy

(Received 18 December 1998)

Electrooptical properties of polymer-dispersed liquid crystals (LCs) are analyzed from the point of view of the order created by the electric field, dynamic changes of the order (orientation) parameter, and optical transmittivity. Optical phase retardation causes an optical phase shift and is related to thermal effects. Nonlinear optical properties are investigated from the point of view of self-transparency, nonlinear gratings, threshold degenerate wave mixing, optical bistability and second harmonic generation.

Keywords: Electrooptical properties; polymer-dispersed liquid crystals; orientation parameter; optical transmittivity; optical phase retardation; nonlinear optical properties; self-transparency; nonlinear gratings; threshold degenerate wave mixing; optical bistability; second harmonic generation

1. INTRODUCTION

In the last years a great scientific interest has grown in polymer Dispersed Liquid Crystals (PDLC), a new class of composite materials consisting of droplets of a low molecular weight liquid crystal dispersed in a polymeric matrix. The droplets are randomly distributed in the polymer and may have a size close to the visible wavelength, thus producing a strong scattering of the incident light. A large variety of structures are possible, depending on the concentration, nature and properties of the polymer and the liquid crystal.

*e-mail: france@anvax1.unian.it

These optoelectronic materials exhibit unique linear and nonlinear optical properties [1] which are expected to expand the liquid crystal technology, in particular into new display and light shutter applications. The principle of operation is based upon the field-controlled light scattering by the liquid crystal microdroplets. In fact, while the polymeric matrix acts as an isotropic solid binder, the droplets exhibit a strong optical anisotropy which depends on the orientation of the liquid crystal inside them. Such orientation can be easily controlled by an external electric or magnetic field. Then, it is possible to reduce the refractive index mismatching between liquid crystal droplets and polymeric matrix by simply applying an electric field of modest intensity (of the order of 10^4 V/cm) to a film of this material, thus switching the sample from the opaque highly scattering state to the transparent highly transmissive state. Submillisecond switching times are possible. This effect is the basis of many applications at present studied such as large-scale flexible displays, high intensity projection television, switchable windows, optical processing and computing devices, thermal sensors and so on, all characterized by being simple and cost effective to fabricate.

Thermally switched films are also prepared with these materials by matching the refractive index of the polymer with that of the liquid crystal in the isotropic phase. A change of the temperature of the film through the nematic–isotropic phase transition reversibly switches the film from opaque to clear.

Another point of extreme interest is that non-linear optical effects can be relevant in these materials.

Besides the technological aspect, PDLC are also very interesting from a fundamental point of view because of many physical problems, some of them being still unsolved, which are strictly connected to the confinement of the liquid crystal in a small cavity. Some of the these problems concern the light propagation through a composite material, the dielectric properties and the local field of the droplets, the reorientational dynamics of the liquid crystal inside the droplet, the dependence of the macroscopic measured parameters on the shape and distribution of the droplets, the role played by the polymer-liquid crystal interfacial interaction because of the very high surface to volume ratio in the liquid crystal droplet.

2. STRUCTURE OF MATERIALS

Dispersion of low molecular weight liquid crystals and polymers give rise to a class of materials which may exist in many forms depending upon the concentrations of polymer, ranging from a few percent to about 70%. The peculiar class of composite materials called PDLC are those of the larger polymer concentration where the liquid crystal is separated in the form of droplets of micron or submicron size randomly distributed throughout the polymer.

In general, the dispersion of liquid crystal droplets within a polymeric matrix can be obtained by means of different technological processes. One of these involves microencapsulation of emulsified nematic droplets with a polymer shell followed by binding to a polymer matrix. Another one is realized through an emulsion of nematic liquid crystal in a water-borne polymer; this aqueous phase can contain a water soluble or a water insoluble polymer and can be coated on a substrate and used like a special ink. Differently from these, the PDLC are self-sustained heterogeneous materials; they may or may not be coated on boundary substrates.

To prepare a PDLC sample the phase separation process is typically used, starting from a homogeneous mixture of a liquid crystal with a fluid prepolymer. The advantage of this technique with respect to others is the possibility of adjusting the droplets size over a wide range (between 0.01 and 20 μm in diameter). Different methods can be used to induce the phase separation between liquid crystal and polymer [2, 3] and the actual procedure used is very important in determining the overall properties of the sample.

The *Polymerization Induced Phase Separation* (PIPS) method is used when the prepolymer is miscible with a low molecular weight liquid crystal, thus forming a homogeneous mixture. The polymerization may start in different ways. When epoxy resins are used, it is achieved through a condensation relation. During the polymerization process the solubility of liquid crystal decreases until a complete separation occurs with the consequent formation of droplets. The shape and size of the droplets are then fixed by the gelation of the polymer and strongly depend on the overall time elapsed between the starting of the droplets nucleation and the gelation of the polymer. When the

polymer is an epoxy resin (like for instance a common epoxy two components glue) which needs the mixing with a curing material at a controlled temperature, the polymerization occurs during the curing process. The size and density of the droplets are then determined by the concentration of the curing material and the curing temperature, besides other important parameters such as the nature of the mixing components, the viscosity of the polymer, the solubility and the diffusion rate of the liquid crystal in the polymer. In same cases, the polymerization process can be induced by absorption of ultraviolet (UV) light rather than by a chemical agent. This occurs when the prepolymers consists of UV curable adhesives. Also this technique in general allows one to obtained satisfactory results.

The *Thermally Induced Phase Separation* (TIPS) method is used with thermoplastic polymers which melt below their decomposition temperature. In this case it is possible to dissolve a liquid crystal in the melt of the polymer and the phase separation takes place when the homogeneous solution is cooled. With this technique the cooling rate is a fundamental parameter in determining the size of the droplets.

Finally, in the *Solvent Induced Phase Separation* (SIPS) method, the liquid crystal and the polymer are both dissolved in the same solvent to produce a homogeneous solution. The solution is then coated on a substrate and after that the solvent is removed by evaporation with the consequent phase separation and polymer solidification. In this case the droplets size is strongly affected by the solvent removal rate.

We observe that mechanical actions on the mixture during the polymerization process may strongly affect size, shape and distribution of the droplets. For instance, stretching along a given direction produces elongated droplets which gives peculiar polarizing properties to the sample.

The anisotropic properties of the nematic liquid crystal droplets originate in the orientation disorder of the molecules. If the molecules are assumed to possess cylindrical symmetry, the macroscopic magnetic susceptibility in the uniform homogeneous bulk phase can be written as

$$\chi_{\alpha\beta} = \rho \frac{(\chi_{\parallel} + 2\chi_{\perp})}{3} \delta_{\alpha\beta} + \rho \frac{2(\chi_{\parallel} - \chi_{\perp})}{3} \left\langle \frac{1}{2} (3m_{\alpha}m_{\alpha} - \delta_{\alpha\beta}) \right\rangle \qquad (1)$$

where **m** is a unit vector along the symmetry axis, ρ is the number density and the brackets $< >$ denotes the ensemble average. A

suitable order parameter to describe nematic order of symmetric molecules is the tensor order parameter Q defined as the anisotropic part of the magnetic susceptibility tensor

$$Q_{\alpha\beta} = \left\langle \frac{1}{2}(3m_\alpha m_\alpha - \delta_{\alpha\beta}) \right\rangle \tag{2}$$

The symmetric traceless tensor $Q_{\alpha\beta}$ can be diagonalized and written in terms of the components of the eigenvectors; if the phase is uniaxial, it reduces to

$$Q_{\alpha\beta} = s\frac{1}{2}(3n_\alpha n_\beta - \delta_{\alpha\beta}) \tag{3}$$

where $\mathbf{n}$ is the nematic director and s is the scalar order parameter defined as

$$s = \frac{1}{2}\langle (3(\mathbf{n}\cdot\mathbf{m})^2 - 1)\rangle = \langle P_2(\mathbf{n}\cdot\mathbf{m})\rangle \tag{4}$$

where $P_2(x)$ is the second order Legendre polynomial. The director $\mathbf{n}$ gives the direction of average orientation of the symmetry axes of the molecules whereas s gives a measure of the degree of orientational order. The tensor order parameter $Q_{\alpha\beta}$ takes into account the overall orientational order by combining the molecular orientational order, described by s, and the director orientation, included in the product $\mathbf{n}_i\mathbf{n}_j$.

The peculiar optical properties of PDLC are due to droplets whose dimensions are of the order of the wavelength of the incident light and in the following we will mainly deal with these droplets and in particular with their effects on the light propagation. At this scale of interest, the droplet can be considered as a whole, *i.e.*, as a single anisotropic particle. Once characterized this particle, the further step involves the consideration of the effects of a large number of droplets uniformly dispersed in the homogeneous matrix, whose orientation and distribution determine the physical properties of the material.

When droplets of micron and over micron size are considered, we can assume that the length scale of spatial variations of the director is much greater than a molecular length, and therefore the director $\mathbf{n}(\mathbf{r})$ can be unambiguously determined at each point $\mathbf{r}$ in the liquid

crystalline inclusions. Then, the classical continuum theory can be applied to study the response of the confined liquid crystal to an external field. Within this frame, the collective properties of the liquid crystal are described by considering the medium as a continuum so that the macroscopic physical properties vary according to the local orientation of the director vector field $\mathbf{n}(\mathbf{r})$. The macroscopic response is known when the orientational distribution of the director $\mathbf{n}$ is known under the particular experimental condition.

The starting point in understanding the physics of PDLC is the director configuration of a nematic liquid crystal when confined to a polymer cavity. Under confinement of micrometer size cavities, the large elastic distortion energies imposed by the curvature of the cavity strongly compete with the molecular anchoring energies at the cavity walls to create a rich variety of director configurations. The stable director configuration inside micron and over micron size nematic droplets in the absence of any external excitation (such as electric or magnetic fields) is a problem which has been widely addressed in the past. This stable configuration is determined from the elasticity of the medium and the boundary conditions through the minimization of the elastic Gibbs function density A_K written in the usual form given by Frank [4]

$$A_K = \frac{1}{2}K_1(\nabla \mathbf{n})^2 + \frac{1}{2}K_2(\mathbf{n} \cdot \nabla \times \mathbf{n})^2 + \frac{1}{2}K_3(\mathbf{n} \times \nabla \times \mathbf{n})^2 \qquad (5)$$

where K_1, K_2, K_3 are the elastic constants for splay, twist and bend, respectively. In the one elastic constant approximation, $K_1 = K_2 = K_3 = K$ and Eq. (5) reduces to

$$A_K = \frac{1}{2}K\{(\nabla \mathbf{n})^2 + (\nabla \times \mathbf{n})^2\} \qquad (6)$$

By assuming a cylindrical coordinate system where θ_n is the angle between the orientation of the local director and the symmetry axis of the droplet, the minimization of Eq. (6) leads to the following non-linear partial differential equation

$$\nabla^2 \theta_n - (1/\mathbf{r}^2)\cos\theta_n \sin\theta_n = 0 \qquad (7)$$

Equation (7) can be solved by the over relaxation method [5]. Several different director configurations are found as possible solutions,

depending on the boundary conditions imposed by the anchoring on the surface of the droplets. Some of these, corresponding to the case of tangential and normal anchoring are shown in Figures 1a and 1b, respectively. All these configurations have been experimentally observed by optical microscopy in droplets sized more than a few microns [6].

A more complex situation occurs when the one elastic approximation does not hold, *i.e.*, when the difference between the elastic constants are not negligible. In these cases, it is possible to observe an

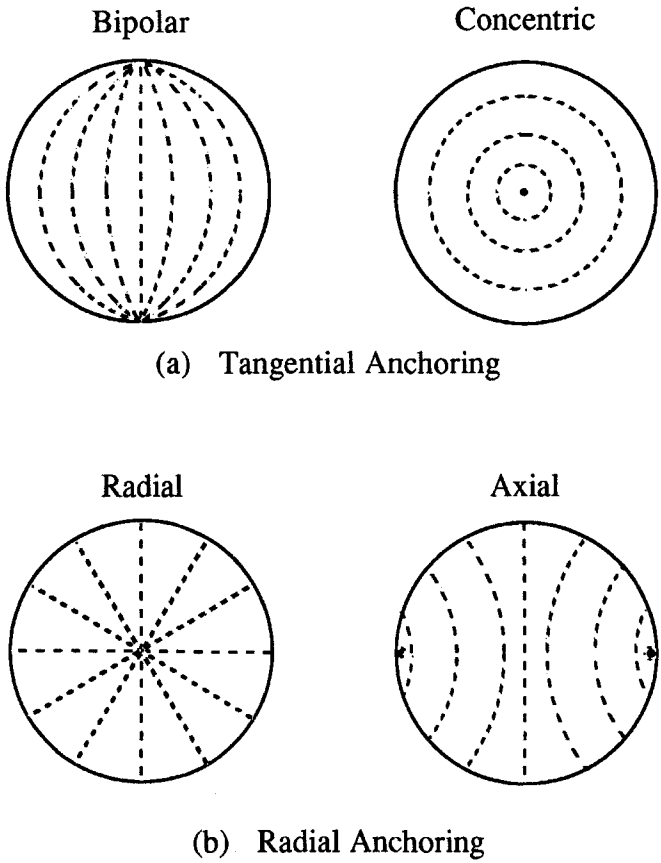

FIGURE 1 Stable nematic director-field configurations in spherical droplets for (a) tangential and (b) radial (perpendicular) anchoring directions at the cavity wall in the strong anchoring limit.

axial alignment even for tangential anchoring [7] when the ratio K_3/K_1 is sufficiently small, and also transitions from bipolar to radial configuration and *vice versa* may occur [8].

In the presence of an external field, the identification of the stable director-field configuration requires the determination of the elastic free energy supplemented by the applied field. This point for the case of the electric field is considered in detail in the following paragraph.

3. ELECTROOPTICAL PROPERTIES

3.1. Electric Field-induced Order

The optical properties of PDLC with droplet size close to the light wavelength are dominated by the light scattering. In the absence of an external electric field, the liquid crystalline droplets are randomly oriented and the incident light probes a range of refractive index values between $n_\perp$ and $n_\parallel$, *i.e.*, the ordinary and extraordinary refractive index of the liquid crystal, respectively. In this state the refractive index mismatching between droplets and polymeric matrix produces a strong light scattering which gives the sample a translucent white appearance (opaque state, see Fig. 2a). When an electric field of sufficient intensity is applied, the molecules in the droplets are collectively reoriented with their director axes parallel to the applied field. This reduces the refractive index mismatching to values that are very close to zero if a proper choice of the compounds is made (*i.e.*, if $n_\perp$ is close to the refractive index of the polymer matrix); the sample is thus switched to a transmission state and it becomes transparent (Fig. 2b).

The application of an electric field to a PDLC sample produces a modification of the director configuration within the nematic droplets. In the general case, this modification consists both in the alignment of the director along a specified direction, which is expected to be the direction of the electric field in the case of a positive dielectric anisotropy ($\Delta\varepsilon > 0$) of the liquid crystal, and a change of the director distribution within the droplet, this latter being strongly dependent on the starting symmetry of the droplet. Calculations performed to determine the liquid crystal configuration (by assuming spherical droplets and infinite anchoring energy) showed that the latter effect is

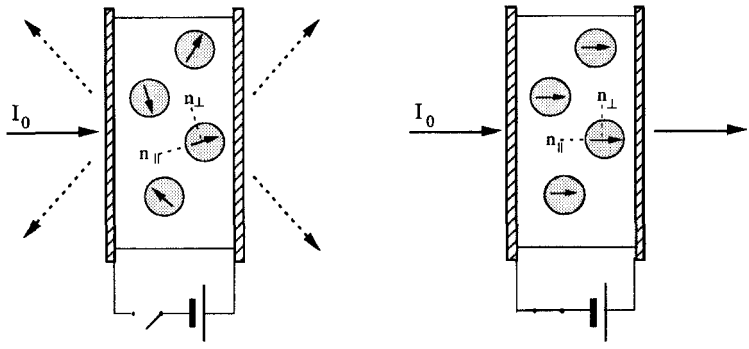

(a) opaque state (b) clear state

FIGURE 2 Principle of operation of a PDLC light shutter based on the applied field controlled light scattering from the liquid crystal microdroplets. (a) OFF state. In the absence on the electric field, the droplets of nematic liquid crystal scatter light in their relaxed randomly aligned state. This is due to the mismatch of the refractive index of the liquid crystal and the polymer binder. The film is opaque; (b) ON state. The external electric field applied normally to the film of PDLC will orient the directors parallel to the field and normal to the surface. Light incident normally to the film plates interacts with the ordinary refractive index $n_\perp$ of the liquid crystal and if the refractive index n_p of the polymer matrix is matched to $n_\perp$ (*i.e.*, $n_p - n_\perp$), the film becomes completely transparent.

negligible in the case of bipolar droplets whereas strong modifications of the internal bipolar configurations are possible in the case of normal anchoring, with possible transitions from radial to axial ones. However, the non-spherical shape of the droplets and the finite value of the anchoring energy actually may result in an effective change of configuration even for bipolar droplets.

The determination of the exact liquid crystal configuration under the application of an external field is a difficult task even for the simplest geometries and becomes prohibitively difficult for PDLC. The approximate approach considered in the following to describe the optical response of PDLC is based upon the assumption that while the applied field reorients the liquid crystal in the inclusions it does not otherwise affect appreciably its internal configuration.

The starting point in determining the effects of an electric field **E** on PDLC is to work out the contribution to the free energy density due to the interaction of the nematic liquid crystal with the electric field. The anisotropic nature of the liquid crystal results in an anisotropic

dielectric permittivity $\underline{\varepsilon}$ which is usually written as

$$\varepsilon_{\alpha\beta} = \varepsilon_{\perp}\delta_{\alpha\beta} + \Delta\varepsilon\, n_{\alpha}n_{\beta} \tag{8}$$

where $\varepsilon_{\parallel}$ and $\varepsilon_{\perp}$ are the elements of the dielectric permittivity parallel and perpendicular, respectively, to the director $\mathbf{n}$ and $\Delta\varepsilon = \varepsilon_{\parallel} - \varepsilon_{\perp}$ is the permittivity (or dielectric) anisotropy. Then, using the definition of dielectric induction

$$\mathbf{D}_{\alpha} = \varepsilon_{\alpha\beta}E_{\beta} = \varepsilon_{\perp}\delta_{\alpha\beta}E_{\beta} + \Delta\varepsilon\, n_{\alpha}n_{\beta}E_{\beta} \tag{9}$$

or, equivalently

$$\mathbf{D} = \varepsilon_{\perp}\mathbf{E} + \Delta\varepsilon(\mathbf{n}\cdot\mathbf{E})\mathbf{n}, \tag{10}$$

the energy density due to the interaction with the field can be written as:

$$U_E = -\frac{1}{4\pi}\int \mathbf{D}\cdot d\mathbf{E} = -\frac{1}{8\pi}\int \varepsilon_{\alpha\beta}E_{\alpha}E_{\beta} = -\varepsilon_{\perp}\frac{E^2}{8\pi} - \frac{\Delta\varepsilon}{8\pi}(\mathbf{n}\cdot\mathbf{E})^2 \tag{11}$$

Accordingly, the additional term in the Gibbs function density, A_E, due to interaction with the electric fields is

$$A_E = -\frac{1}{8\pi}\Delta\varepsilon(\mathbf{E}\cdot\mathbf{n})^2 \tag{12}$$

where the contribution associated to the isotropic part of the permittivity has been omitted because it does not depend on the director orientation. Most nematic liquid crystals exhibit positive dielectric anisotropy and Eq. (12) indicates that they tend to align with the director $\mathbf{n}$ parallel to the applied $\mathbf{E}$.

In evaluating F_E by means of Eq. (12) we must observe that $\mathbf{E}$ represents the electric field inside the droplet. This is an important problem since, due the composite nature of the PDLC material and the dielectric anisotropy of the liquid crystal, the effective field inside the droplet is in general very different from the applied external one. On the other hand, the exact determination of the field distribution throughout the whole sample is an enormously difficult task. A simple way to overcome this problem, even if in an approximate form, is to consider the classical problem of an isolated spherical droplet

embedded in a uniform electric field. In this case, the classical electrostatic boundary condition gives [9]

$$\mathbf{E} = \mathbf{E}_p \frac{3\varepsilon_p}{2\varepsilon_p + \varepsilon_d} \tag{13}$$

where $\mathbf{E}$ is the electric field inside the droplet (the local field) and the suffixes p and d stand for polymer binder and droplet, respectively. We observe that Eq. (13) is only an approximate expression which makes it possible to estimate the local field once known the external field $\mathbf{E}_p$. This latter, on its turn, does not coincide with the applied field.

A more accurate relation should take into account also the liquid crystal anisotropy which makes ε_d a function of both $\varepsilon_\parallel$ and $\varepsilon_\perp$.

By considering the finite conductivity σ of both the polymer and the liquid crystal and introducing the complex dielectric permittivity $\varepsilon = \varepsilon' + i\sigma/\omega$, Eq. (13) can be written, in the low frequency limit ($\omega \to 0$), as

$$\mathbf{E} = \frac{3\mathbf{E}_p}{\sigma_d/\sigma_p + 2} \tag{14}$$

Being typically the conductivity of the liquid crystal much stronger that the one of the polymer ($\sigma_d \gg \sigma_p$), the last equation clearly shows that the electric field inside the droplet is much weaker that the external one. This is actually the main obstacle to the droplet reorientation in the case of weak applied electric fields.

Different approaches, depending on the size of the droplets and the experimental technique, are available in the literature to analyze the response of PDLC to low frequency electric fields. Since we are interested in the optical properties of PDLC we are mainly concerned with submicron size droplets where the bipolar configuration is known to be generally the most stable one. The analysis reported in the following to describe the electro-opticl response of PDLC made of bipolar droplets follows the optical and dielectric response of these materials to the external fields *via* their effect on a hierarchy of order parameters.

A *scaling* of the classical description of nematic liquid crystals to the droplet scale allows to introduce new order parameters which describe the degree of orientational order of the droplets. We define the droplet director $\mathbf{N}_d$ as the unitary vector which gives the average orientation of the nematic director $\mathbf{n}$ within the droplet. In the absence of external fields, the direction of $\mathbf{N}_d$ coincides with the symmetry axis of the droplet.

Then, in analogy with the scalar order parameter s of nematics (Eq. (4)), we introduce the scalar droplet order parameter s_d defined as

$$s_d = \frac{1}{2}\langle(3(\mathbf{N}_d \cdot \mathbf{n})^2 - 1)\rangle_{V_d} = \langle P_2(\mathbf{N}_d \cdot \mathbf{n})\rangle_{V_d} \tag{15}$$

to give a measure of the degree of orientational order of the nematic director in the volume V_d of the droplet. Droplet order parameters have been calculated for a variety of director configurations [11] and examples are shown in Figure 3.

Finally, the symmetric traceless tensor order parameter Q_d of the droplet is defined as the volume average of the tensor order parameter Q over the droplet

$$(Q_d)_{\alpha\beta} = (1/V_d)\int_{V_d} Q_{\alpha\beta}(\mathbf{r})d^3\mathbf{r} \tag{16}$$

If Q_d is uniaxial, that is if two of its eigenvalues are identical, then it can be written in terms of the eigenvector $\mathbf{N}_d$ associated to the unique eigenvalue λ_d to give (see Eq. (3) for analogy)

$$(Q_d)_{\alpha\beta} = \lambda_d \frac{1}{2}(3N_{d\alpha}N_{d\beta} - \delta_{\alpha\beta}) \tag{17}$$

The eigenvalue λ_d is then

$$\lambda_d = s\frac{1}{2}\langle(\mathbf{N}_d \cdot \mathbf{n})^2 - 1)\rangle_{V_d} = ss_d \tag{18}$$

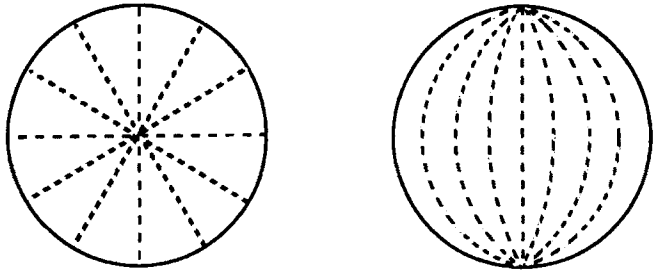

FIGURE 3 Examples of droplet order parameters.

If the liquid crystal order parameter s is constant inside the droplet, as it can be assumed for nematic liquid crystals in the limit of long wavelength distortion of the director field $\mathbf{n}(\mathbf{r})$ [12], then we obtain

$$(Q_d)_{\alpha\beta} = ss_d \frac{1}{2}(3N_{d\alpha}N_{d\beta} - \delta_{\alpha\beta}) \tag{19}$$

The tensor order parameter Q_d gives a complete description of the droplet's order by including the vector $\mathbf{N}_d$, which gives its orientation in space, the quantity s_d, related to the director configuration and the quantity s which measures the effects of the thermal fluctuations. The product ss_d gives the degree of orientational order of the liquid crystal molecules in the droplet.

The droplets are assumed to have a symmetric ellipsoidal shape; this choice has important consequences both on the orientational properties of the liquid crystal director and on its relaxation behavior after removal of the electric field. In fact, besides the consideration that some experimental data actually support the anisotropic slightly ellipsoidal shape of the droplets, a non-spherical shape allows to account for the origin of the torque which restores the initial director configuration after removal of the electric field: it is possible to shown that with such non-spherical shape of the droplet the initial configuration is the one which corresponds to the minimum deformation energy while any director reorientation from the initial state increases the distortion elastic energy. However, an alternative answer to the origin of the restoring torque could be found in the effects of the anchoring at the liquid crystal–polymer interface which gives some additional contribution to the free energy of the droplet making higher the energy of the reoriented configuration. On the basis of these considerations, the ellipticity parameter introduced in the following must be considered as a phenomenological parameter, a sort of *effective* ellipticity which includes both the effects of the shape and the anchoring. In terms of the vector $\mathbf{r}$ from the centre to a point on its surface, the ellipsoid equation may be written as

$$r_\alpha r_\beta \Lambda_{\alpha\beta} = R^2 \tag{20}$$

where R is the average radius of the cavity and $\Lambda_{\alpha\beta}$ is the characteristic tensor of the cavity shape, given by

$$\Lambda_{\alpha\beta} = \delta_{\alpha\beta} - (2/3)\zeta^2(1/2)(3L_\alpha L_\beta - \delta_{\alpha\beta}) \tag{21}$$

where ζ is the eccentricity and $\hat{\mathbf{L}}$ a unit vector along the symmetry axis of the ellipsoid (see Fig. 4). In the absence of electric fields the droplet director $\mathbf{N}_d$ is parallel to $\hat{\mathbf{L}}$. When an electric field is applied, the elastic free energy is expected to be proportional to $(\mathbf{N}_d \cdot \hat{\mathbf{L}})^2$. Kelly and Palffy – Muhoray [10] proposed the following expression for the elastic Gibbs function per volume

$$A_k = \frac{K}{R_c^2}\left\{1 + \frac{1}{3}a(Q_d)_{\alpha\beta}\Lambda_{\alpha\beta} + \cdots\right\} \tag{22}$$

where a is a constant and R_c^{-2} given by

$$(1/R_c)^2 = \langle(\nabla \mathbf{n})^2 + (\nabla \times \mathbf{n})^2\rangle V_d \tag{23}$$

is the mean squared cuvature of the director field in the cavity. The first term on the right hand side of Eq. (22) does not depend on the orientation of the droplet director and represents the elastic free energy density of the liquid crystal in the spherical inclusion while the second term is the contribution of the non-spherical shape of the cavity. The higher order terms in the expansion (22) corresponds to higher order moments of the cavity shape. Ignoring the first term,

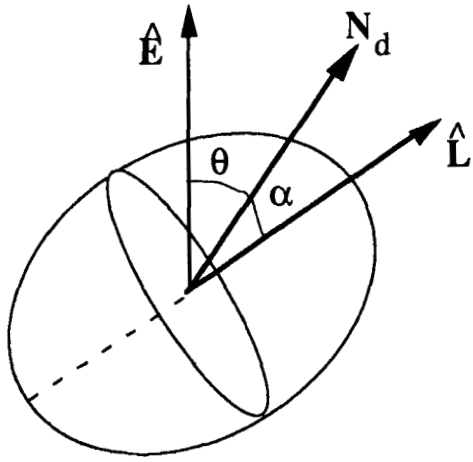

FIGURE 4 Ellipsoidal droplet in an external electric field $\mathbf{E}$. $\hat{\mathbf{E}}$ is the unit vector giving the direction of the electric field, $\mathbf{N}_d$ is the droplet director and $\hat{\mathbf{L}}$ is the unit vector along the symmetry axis of the ellipsoid.

which does not play any role in determining the stable configuration, and letting $a/R_c^2 = 1/R_{\text{eff}}^2$, one gets

$$A_k = -\frac{1}{3}\frac{K}{R_{\text{eff}}^2}\zeta^2 s s_d P_2(\hat{\mathbf{L}} \cdot \mathbf{N}_d) \tag{24}$$

This result is confirmed by more detailed calculations for a number of director configurations.

The electric field applied to a PDLC sample tends to orient the droplet director along the direction of the field. However, this alignment process is hindered by the elastic forces. In analogy to the previous definitions of the scalar order parameters s and s_d, we may introduce a new scalar order parameter s_E, which we call the sample order parameter, suitable to describe the degree of alignment of a PDLC sample when subjected to an electric field and defined as

$$s_E \equiv \langle P_2(\mathbf{N}_d \cdot \hat{\mathbf{E}}) \rangle_{V_f} \tag{25}$$

where $\hat{\mathbf{E}}$ is the unit vector giving the direction of the electric field $\mathbf{E}$ and V_f is the overall volume of the sample. The elastic free energy density F_E due to the interaction with the electric field (Eq. (12)) can then be expressed in terms of s_E. However, the exact calculation of F_E is enormously difficult as the free energy density of each droplet cannot be considered independently because of the interactions among the droplets occurring *via* strong depolarizing fields. To simplify the calculation it is used the so called *effective medium* approximation which has proven to be efficacious to describe the dielectric constant of these systems [13]. Within this approach the actual PDLC sample is replaced by a homogeneous sample with the same dielectric characteristics. The effective dielectric constant ε_m of the this homogeneous medium is given by

$$\varepsilon_m = \varepsilon_p + 3v_{\text{lc}} \frac{\varepsilon_p(\varepsilon_{\text{lc}} - \varepsilon_p)}{\varepsilon_{\text{lc}} + 2\varepsilon_p - v_{\text{lc}}(\varepsilon_{\text{lc}} - \varepsilon_p)} \tag{26}$$

where v_{lc} is the volume fraction of the liquid crystal in the sample, ε_p is the dielectric constant of the polymer and ε_{lc} is the average dielectric constant of the liquid crystal (averaged over the sample) in response to a unitary applied field $\hat{\mathbf{E}}$, *i.e.*, $\varepsilon_{\text{lc}} = \langle \hat{\mathbf{E}} \underline{\varepsilon} \hat{\mathbf{E}} \rangle_{V_f}$. Assuming that the liquid crystal is present only inside the droplets considered identical and with

constant order parameter s_d one obtains [14]

$$\varepsilon_{lc} = \varepsilon_\perp + \frac{1}{3}\Delta\varepsilon(1 + 2ss_d s_E) \tag{27}$$

The Helmholtz function $A'_{f,E}$ of the overall sample due to interaction with the electric field can be written as

$$A'_{f,E} = -(1/2)\varepsilon_m E^2 V_f \tag{28}$$

In order to find the stable configuration by minimization of the overall Helmholtz function density, it is sufficient to consider in the last equation only the term depending on the liquid crystal orientation. Assuming uniform droplets so that the droplet volume is simply $V_d = v_{lc}V_f/N$ (N is the number of droplets), this term can be written as

$$\begin{aligned} A'_{f,E} &= -(1/3)\Delta\varepsilon E^2 V_f v_{lc} s s_d g(s_E) s_E = \\ &= -(1/3)\Delta\varepsilon E^2 V_d s s_d g(s_E) \sum_i P_2(\hat{\mathbf{E}} \cdot \mathbf{N}_d^{(i)}) \end{aligned} \tag{29}$$

where

$$g(s_E) = \frac{3\varepsilon_p}{\varepsilon_{lc} + 2\varepsilon_p - v_{lc}(\varepsilon_{lc} - \varepsilon_p)} \tag{30}$$

which is a function of s_E through ε_{lc}. The Helmholtz function for a single droplet is then

$$A'_E = -(1/3)\Delta\varepsilon E^2 V_d s s_d g(s_E) P_2(\hat{\mathbf{E}} \cdot \mathbf{N}_d) \tag{31}$$

and the Helmholtz function density

$$A_E = A'_E/V_d = -(1/3)\Delta\varepsilon E^2 s s_d g(s_E) P_2(\hat{\mathbf{E}} \cdot \mathbf{N}_d) \tag{32}$$

The total Helmholtz function density dependent on the droplet orientation is obtained by summing the two contributions coming from Eqs. (24) and (32)

$$\begin{aligned} A = A_E + A_k = &-\frac{1}{3}\frac{K}{R_{\text{eff}}^2}\zeta^2 s s_d P_2(\hat{\mathbf{L}} \cdot \mathbf{N}_d) \\ &-\frac{1}{3}\Delta\varepsilon E^2 s s_d g(s_E) P_2(\hat{\mathbf{E}} \cdot \mathbf{N}_d) \end{aligned} \tag{33}$$

This equation shows that, to the order of approximation of the present analysis, the effect of the cavity shape on the droplet order parameter is the same as that of an external field. By minimization we get

$$3(\hat{\mathbf{L}} \cdot \mathbf{N}_d)\hat{\mathbf{L}} + 3e^2(\hat{\mathbf{E}} \cdot \mathbf{N}_d)\hat{\mathbf{E}} = \lambda \mathbf{N}_d \tag{34}$$

where λ is the Lagrange multiplier and e

$$e = \left(\frac{R_{\text{eff}}}{\zeta}\sqrt{\frac{g\Delta\varepsilon}{K}}\right)E \tag{35}$$

is the normalized dimensionless expression of the electric field.

According to Eq. (34), the applied field orients the droplet's director $\mathbf{N}_d$ in the plane $\hat{\mathbf{E}}$, $\hat{\mathbf{L}}$. (see Fig. 3). The knowledge of the angle between $\mathbf{N}_d$ and the applied field $\mathbf{E}$ is then sufficient to describe the orientation of a single droplet. This information is obtained by solving Eq. (34) with respect to $P_2(\mathbf{N}_d \cdot \hat{\mathbf{E}})$, which gives

$$P_2(\hat{\mathbf{E}} \cdot \mathbf{N}_d) = \frac{1}{4} + \frac{3}{4}\frac{e^2 - 1 + 2(\hat{\mathbf{E}} \cdot \hat{\mathbf{L}})^2}{[(e^2 - 1)^2 + 4e^2(\hat{\mathbf{E}} \cdot \hat{\mathbf{L}})]^{1/2}} \tag{36}$$

To obtain the actual sample order parameter we must average the sample order parameter of the single droplet over all droplet orientations, *i.e.*,

$$s_E = \frac{1}{4\pi}\int P_2(\hat{\mathbf{E}} \cdot \mathbf{N}_d)d\Omega_L \tag{37}$$

where $d\Omega_L$ is the element of solid angle associated with the orientation of $\hat{\mathbf{L}}$.

Assuming a uniform orientational distribution of the symmetry axes $\hat{\mathbf{L}}$ of the droplets, after some calculations we get

$$s_E = \frac{1}{4} + \frac{3(e^2 + 1)}{16e^2} + \frac{3(3e^2 + 1)(e^2 + 1)}{32e^2}\ln\left|\frac{e + 1}{e - 1}\right| \tag{38}$$

Since e depends on s_E through the quantity g (see Eq. (35)), the last equation provides an implicit expression of s_E which requires a numerical approach to be solved. The expression (38) for the field dependence of the sample order parameter is a very important result. The optical

response of the sample can be expressed in terms of the sample order parameter as well as other ones.

Figure 5 shows the behavior of the sample order parameter s_E as a function of the applied voltage $V(V = Ed$, where d is the thickness of the PDLC sample assumed in the form of a thin film) for $R = 200$ nm, $\zeta = 0.13$, $K = 2{\cdot}10^{-11}$ N, $v_{lc} = 0.5$ and $s_d = 0.7$. The curve increases monotonically with V and approaches asymptotically the saturation value $(s_E)_{max} = 1$. A threshold voltage V_t can be defined as the value of V which corresponds to half the maximum value of the sample order parameter s_E, *i.e.*, to $s_E = (s_E)_{max} = 0.5$.

Figures 6(a–c) show the behavior of V_t as a function of the variable parameter R, ζ, K, respectively. In particular we observe that V_t increases reducing the radius R of the droplet. This result is justified by the consideration that smaller droplets means higher director distortion and hence higher elastic torque which compete with the torque induced by the electric field. A similar effect is observed by increasing the ellipticity ζ or the elastic constant K, which explains the trends of V_t in Figures 6b and 6c.

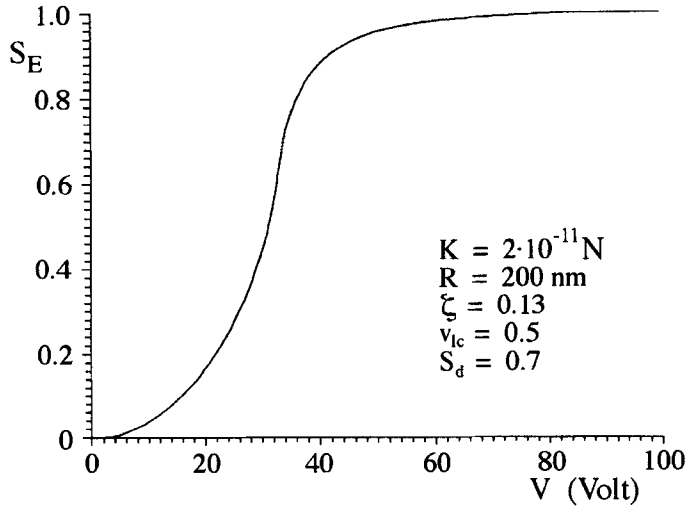

FIGURE 5 The sample order parameter s_E as a function of the applied voltage V for fixed values of the parameters R, ζ, K, v_{lc} and s_d.

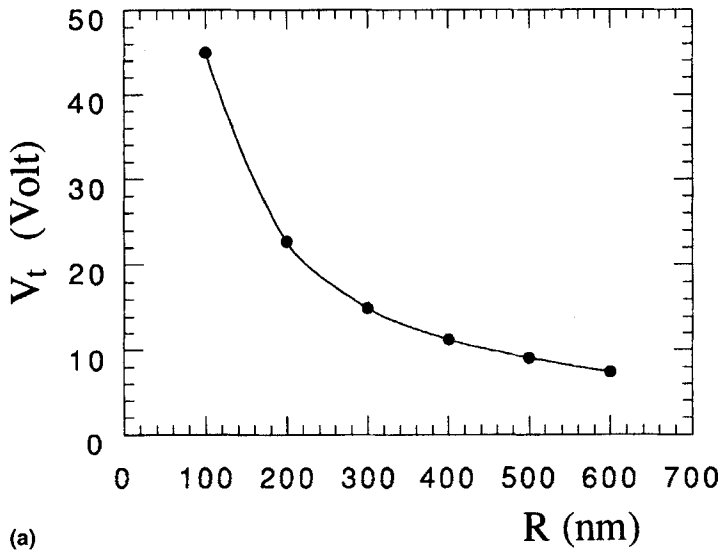

C

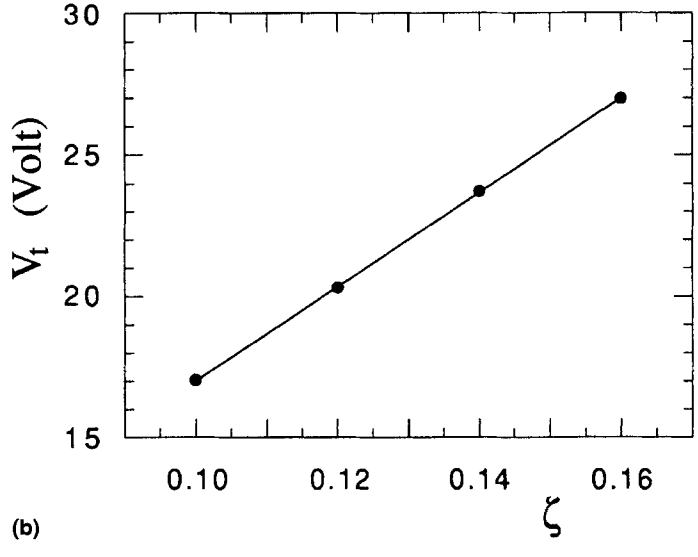

FIGURE 6 The behavior of the threshold voltage V_t as a function of R (a), ζ (b) and K (c). In (a) it is assumed $\zeta = 0.13$ and $K = 10^{-11}$ N, in (b) $R = 200$ nm and $K = 10^{-11}$ N, in (c) $R - 200$ nm $\zeta - 0.13$ whereas for all figures it is $v_{lc} = 0.5$ and $S_d = 0.7$.

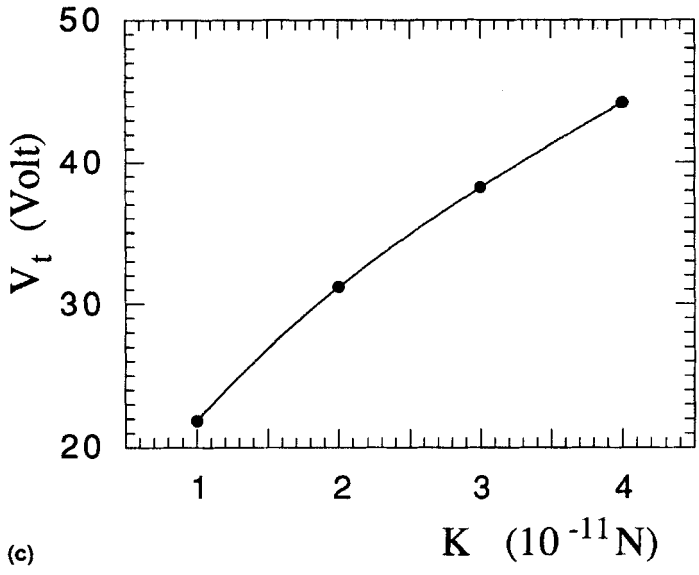

FIGURE 6 (Continued).

The order of magnitude of the electric field E necessary to induce the reorientation of the droplet is easily obtained from Eq. (35) taking $e = 1$ (which means assuming the electric torque equal to the elastic torque)

$$E = \left(\frac{\zeta}{R_{\text{eff}}} \sqrt{\frac{K}{g\ \Delta\varepsilon}} \right) \tag{39}$$

By combining Eqs. (39) and (14) a qualitative estimate of the threshold voltage is then obtained as

$$V_t = \frac{d}{3} \left(\frac{\sigma_d}{\sigma_d} + 2 \right) \left(\frac{\zeta}{R_{\text{eff}}} \sqrt{\frac{K}{g\Delta\varepsilon}} \right) \tag{40}$$

which is in good agreement with the trends shown in Figures 6.

3.2. Order Parameter Dynamics

The dynamical response of PDLC to time dependent electric fields is a subject of considerable interest especially because of the possible technological applications of these materials. It can be studied by

considering the torque T acting on the liquid crystal in the droplets, given by

$$T = T_K + T_E = -\frac{\partial A_K}{\partial \theta} - \frac{\partial A_E}{\partial \theta} = -\frac{\partial F}{\partial \theta} \tag{41}$$

where $T_k = -\partial F_K/\partial\theta$ and $T_E = -\partial F_E/\partial\theta$ are the elastic and electric torque, respectively, and θ is the angle between the droplet director $\mathbf{N}_d$ and the applied field $\mathbf{E}$. If the droplet is assumed to behave as a rigid body, its rotational motion is governed by the equation

$$-\frac{\partial F}{\partial \theta} - \Gamma\frac{d\theta}{dt} = I_d\frac{d^2\theta}{dt^2} \tag{42}$$

where I_d is the momentum of inertia of the droplet and a viscous damping term is considered which accounts for the dissipation of mechanical energy caused by friction during the rotation. The viscosity coefficient Γ is the average of the viscosity coefficients associated to the elastic deformations (primarily bend and splay in the case of bipolar droplets). Actually, in most cases the term proportional to the second derivative of θ is negligible due to the smallness of I_d. In these cases, after renormalization and considering Eq. (33) for F, the equation of the motion can be explicitly written as [14]

$$\tau\frac{\partial\theta}{\partial t} = -\frac{1}{2}[\sin 2(\theta - \xi) + e^2 \sin 2\theta] \tag{43}$$

where ξ is the fixed angle between the symmetry axis $\hat{\mathbf{L}}$ of the ellipsoidal cavity and the electric field $\mathbf{E}$ and τ is the characteristic time constant of the droplet defined as

$$\tau = \frac{\Gamma R_{\text{eff}}^2}{K s s_d \zeta^2 V_d} \tag{44}$$

Once specified the experimental conditions, in particular the time dependence of $e(t)$, the dynamic response $\theta(t)$ of the single droplet is determined by solving the differential Eq. (43) with the appropriate initial conditions. The time dependent sample order parameter $s_E(t)$ is then obtained by averaging the single droplet orientational parameter $P_2(\hat{\mathbf{E}}\cdot\mathbf{N}_d) = P_2[\cos\theta(t)]$ over all droplet orientations.

If the applied field vary very slowly, the viscous torque can be neglected and the dynamic response is quasi static with the constant field e replaced by the time dependent $e(t)$.

Two situations of practical relevance are those when a constant electric field e_0 is instantaneously applied or removed at a given time $t = 0$. In the first case, after writing Eq. (43) in the form

$$\frac{\partial \theta}{\partial t} = -\frac{1}{2\tau}\frac{\sin 2\xi}{\sin 2\gamma}\sin 2(\theta - \xi) \tag{45}$$

where

$$\sin 2\gamma = \frac{\sin 2\xi}{\sqrt{\sin^2 2\xi + (e_0^2 + \cos 2\xi)^2}} \tag{46}$$

the integration of Eq. (45) with the initial condition $\theta(0) = \theta_0$ gives

$$\tan(\theta - \xi) = \tan(\theta_0 - \xi)\exp\left(-\frac{t}{\tau}\frac{\sin 2\xi}{\sin 2\gamma}\right) \tag{47}$$

The time constant $\tau_{ON} = \tau \sin 2\gamma / \sin 2\xi$ in the exponential function measures the rapidity of the response of the droplet to the applied electric field. We call it the *switch-on* time constant of the single droplet. The switch-on time constant of the overall sample can be obtained from this latter through an averaging procedure which involves the calculation of the time dependent sample order parameter $s_E(t)$. In the case of a uniform orientational distribution of the symmetry axes of the droplets, the parameter $s_E(t)$ can be calculated by Eq. (37) and the result of the integration is [10]

$$s_E(t) = -\frac{1}{2} + \frac{3}{8\pi}\int_{\Omega_L} \frac{(1 - \tan(\theta - \xi)\tan\xi)^2}{(1 + \tan^2(\theta - \xi))(1 + \tan^2\xi)} d\Omega_L \tag{48}$$

In the second relevant situation, when the electric field is suddenly removed at $t = 0$, we have $e = e_0 = 0$ in Eq. (41) and the initial condition $\theta(0) = \theta_{max}$. Integration of Eq. (43) gives then

$$\tan(\theta - \xi) = \tan(\theta_{max} - \xi)\exp\left(-\frac{t}{\tau}\right) \tag{49}$$

This equation shows that the difference $\theta - \xi$ approaches zero with a *switch-off* time constant τ_{OFF} equal to τ. Then, τ gives a measure of the relaxation time necessary to restore the starting orientation of a single droplet when the field is turned off. By comparing τ_{ON} and τ_{OFF} we observe that, being $\sin 2\gamma \leq \sin 2\xi$ (see Eq. (37)), τ_{ON} is always smaller than τ_{OFF} and the two constants become coincident ($\tau_{ON} = \tau_{OFF} = \tau$) in the limit as the applied field approaches zero. A special case of considerable importance in when the initial distribution of the droplets (before turning off the electric field) corresponds to a unitary sample order parameter, *i.e.*, $s_E(0) = 1$, which means that all the droplet directors are exactly aligned along the direction of the electric field. In principle we may think to meet such a configuration when a sufficiently strong electric field is applied to the PDLC sample. In this case, the optical transmittivity of the PDLC decreases with time as the directors relax to the zero field equilibrium state and such decay is an important property for light shuttering applications. The solution for the $\theta - \xi$ time dependence is given by Eq. (49) with $\theta_{max} = 0$. Then, integration of Eq. (48) gives

$$s_E = 1 - \frac{1}{(1+U)^2}\left[1 + \frac{3U^2}{2} - \frac{3U}{2\sqrt{1-U^2}}\tan^{-1}\left(\frac{\sqrt{1-U^2}}{U}\right)\right] \tag{50}$$

where $R = \exp(-t/\tau)$. Unlike the response of a single droplet, the decrease of order is not simply exponential, except at times $t \gg \tau$.

The above results can be easily extended to the case of a sinusoidal electric field $e(t) = e_0 \cos(\omega t)$. In this case we can write $\theta(t) = \theta_0 + \Delta(t)$, where θ_0 is the average direction about which the droplets directors oscillate in the period $T = 2\pi/\omega$. If T is chosen such that $T \ll \tau$, the equation of the motion (43) can be written, to the lowest order in Δ,

$$\tau \frac{\partial \Delta(t)}{\partial t} = -\frac{1}{2}[\sin 2(\theta_0 - \xi) + e^2 \sin 2\theta_0] \tag{51}$$

which, after averaging both sides, gives

$$\sin 2(\theta_0 - \xi) + \langle e^2 \rangle \sin 2\theta_0 = 0 \tag{52}$$

This is the same equilibrium equation which holds for a constant field, with the only difference that the constant field e is replaced by its root mean square value.

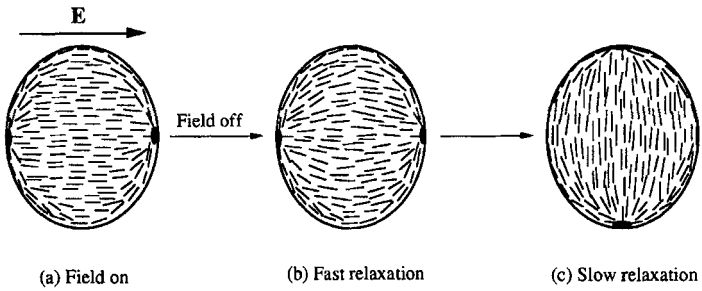

FIGURE 7 Model for the two stage decay time response in PDLC films. (b) The first temporal decay upon removal of the electric field is ascribed to a simple realignment of the director field within the droplet (while the droplet director remains unchanged). (c) The following slow decay involves the reorientation of the droplet director to the configuration it possessed prior to application of the field. This process requires both the movement of the nematic surface layer and a rotation of the nematic within the bulk of the droplet.

In some experiments [15, 16], two characteristic exponential decay times, a fast one (0.1–0.1 ms) and a slow one (10–1000 ms), were observed in the transmission *vs.* time curve after removal of the external applied voltage. In the model proposed by Drzaic [16] to explain this behavior, the reorientation of the nematic droplets takes place in two stages (Fig. 7): a fast reorientation by the nematic within the bulk of the droplet, followed by a slower rotation of the nematic nearer the droplet surface, including the point disclinations, which results in a reorientation of the droplet director.

3.3. Optical Transmittivity

The intensity of a light beam of light passing through a PDLC sample is reduced by the scattering due to the liquid crystal droplets. In the regime where the amount of light scattered by the single droplet is small compared to the transmitted light (hence multiple scattering effects are negligible), the intensity $I(d)$ of the beam after a path length d in the sample can be well described [17] by the following exponential decay law

$$I(d) = I(0)e^{-\beta\sigma d} \tag{53}$$

where $I(0)$ is the incident intensity, $\beta = N/V$ (N is the number of droplets and V is the sample volume crossed by the beam) is the number density of droplets and σ is the sample scattering cross section, *i.e.*, the average droplet scattering cross section, averaged over the different droplet orientations ($\sigma = \langle \sigma_d \rangle_s$). If we introduce the liquid crystal volume fraction v_{lc} and the average droplet radius $\langle R_{eff}^3 \rangle^{1/3}$, the number density β can be written as

$$\beta = \frac{v_{lc}}{\frac{4}{3}\pi \langle R_{eff}^3 \rangle} \tag{54}$$

and Eq. (53) becomes

$$I(d) = I(0)e^{-\alpha d} \tag{55}$$

where

$$\alpha = v_{lc} \frac{3\sigma}{4\pi \langle R_{eff}^3 \rangle} \tag{56}$$

We want to determine the transmittivity of PDLC films as a function of the intensity of an electric field applied normally to the film, which is the situation more frequently encountered in practical cases. We consider a plane-polarized beam of monochromatized light with wavelength λ and electric field $\mathbf{E} = \mathbf{E}_0 \exp[i(\mathbf{k} \cdot \mathbf{r} - \omega t)]$, impinging the sample normally to the film plate. In the general case, the cross section σ_d of a given droplet depends on the relative orientations of the three vectors $\mathbf{k}$, $\mathbf{E}_0$ and $\mathbf{N}_d$. In this case, being the projections of the droplet directors onto the plane normal to $\mathbf{k}$ randomly distributed, the droplet cross section will be only a function of the angle θ between $\mathbf{k}$ and $\mathbf{N}_d$ (which in this geometry is also the angle between $\mathbf{N}_d$ and the applied field). Then, expanding in Legendre polynomials, we can write [10]

$$\langle \sigma_d \rangle_E = \sum_{n=0}^{\infty} a_{2n} P_{2n}(\cos\theta) \tag{57}$$

where $\langle \cdots \rangle_E$ denotes the average over the electric field orientations and only even order terms are considered because of the physical equivalence between the directions $\mathbf{N}_d$ and $-\mathbf{N}_d$. The expansion

coefficients depend on the wavelength λ and on the shape, size and director configuration of the droplet. The sample scattering cross section is obtained by averaging over all droplets in the sample

$$\sigma = \sum_{n=0}^{\infty} a_{2n} \langle P_{2n}(\cos\theta) \rangle_s \tag{58}$$

The quantities within brackets in the second member of Eq. (58) are the sample order parameters. Thus, the optical transmittivity, like all the optical properties of PDLC, are strongly related to the sample order parameters. We observe that, in some significant situtations, the first few terms of the expansion are sufficient to give an adequate description of the phenomena.

The theory of light scattering from a single spherical liquid crystal droplet has been developed by Zumer [18] and Zumer and Doane [19]. Within these models, the anisotropic droplet is assumed to be embedded in an isotropic matrix having a comparable refraction index. In addition, the droplet is assumed to behave as an *optically soft* (or weakly refracting) scattering object, *i.e.*, the following condition is considered to hold

$$|(n_{lc}/n_p - 1)| \ll 1 \tag{59}$$

where the subscripts lc and p stand for liquid crystal and polymer, respectively. Since in most cases the two refraction indexes, $n_\perp$ and $n_\parallel$, of the nematic phase differ by at most 15% [20] (taking values between 1.5 and 1.75) and each of the two differs only slightly from the value of the surrounding polymer ($n_p \sim 1.55$), the last condition is generally verified for PDLC samples.

The two following extreme situations were theoretically considered. The first one concerns the scattering from small (submicron) *soft* droplets [19], where the radius R of the droplet is much smaller than the light wavelength λ, *i.e.*, $kR \ll 1$ where $k = 2\pi/\lambda$ is the light wavevector in the medium (as an example, for light with $\lambda = 650\,\text{nm}$ and $n_p = 1.5$ the droplet radius should not exceed $0.1\,\mu\text{m}$). In these conditions, together with Eq. (59) the following holds

$$2kR|(n_{lc}/n_p - 1)| \ll 1 \tag{60}$$

and the use of the Rayleigh–Gans approximation [21–22](RGA) is justified. From a physical point of view, the condition expressed by (60) means that the maximum phase shift induced by a diametral crossing of a droplet is small.

The differential scattering cross section $d\sigma/d\Omega$ is written as

$$\frac{d\sigma}{d\Omega} = \frac{|\mathbf{f}(\mathbf{k}, \mathbf{k}')|^2}{|\mathbf{E}_0|^2} \tag{61}$$

where $\mathbf{k}$ and $\mathbf{k}'$ are the incident and scattered wavevectors, respectively, and $\mathbf{f}(\mathbf{k}, \mathbf{k}')$ is the scattering amplitude which, in the RGA, is given by

$$\mathbf{f}(\mathbf{k}, \mathbf{k}') = \frac{1}{4\pi} V_d k^2 (\mathbf{P} - \hat{\mathbf{i}}'[\hat{\mathbf{i}}' \cdot \mathbf{P}]) \tag{62}$$

where $\hat{\mathbf{i}}' = \mathbf{k}'/\mathbf{k}$, V_d is the droplet volume and

$$\mathbf{P} = \mathbf{E}_0 \cdot \langle (\underline{\varepsilon}_r - \underline{1}) \exp[-i(\mathbf{k}' - \mathbf{k}) \cdot \mathbf{r}] \rangle_d \tag{63}$$

In the last equation the average is performed over the droplet and ε_1 is the relative dielectric tensor given, in its local principal frame, by

$$\underline{\varepsilon}_r = \frac{1}{\varepsilon_p} \begin{bmatrix} \varepsilon_\perp & 0 & 0 \\ 0 & \varepsilon_\perp & 0 \\ 0 & 0 & \varepsilon_\parallel \end{bmatrix} \tag{64}$$

If $kR \ll 1$, the exponential in Eq. (63) approaches a unitary value so that

$$\mathbf{P} = \mathbf{E}_0 \cdot \langle (\underline{\varepsilon}_r - \underline{1}) \rangle_d \tag{65}$$

and the droplet behaves as a radiating dipole with polarizability given by the volume averaged polarizability of the droplet. Separating the dielectric tensor into an isotropic and an anisotropic part, the bracketed term in the last equation can be written as

$$\langle (\underline{\varepsilon}_r - \underline{1}) \rangle_d = \zeta \underline{1} + 2\eta \underline{\mathbf{O}}_d \tag{66}$$

where $\underline{\mathbf{O}}_d$ is the droplet order parameter tensor,

$$\zeta = \frac{1}{3} \mathrm{Tr}(\underline{\varepsilon}_r) - 1 \tag{67}$$

and

$$\eta = \frac{\varepsilon_{\parallel} - \varepsilon_{\perp}}{3\varepsilon_p} \tag{68}$$

The differential scattering cross section $d\sigma/d\Omega$ is determined by calculating the far field scattered by the radiating dipole **P** and the total droplet scattering cross section is then obtained by integration of $d\sigma/d\Omega$ over the whole solid angle

$$\sigma_d = \int_{\Omega} \frac{d\sigma}{d\Omega} d\Omega \tag{69}$$

The theory gives a scattering cross section which can be calculated in a closed form only for particular situations involving a uniform director configuration ($s_d = 1$). In this case, the droplet scattering cross section is found to be

$$\sigma_d^{\mathrm{RGA}} = \sigma_0 \frac{(2kR)^4}{108} [(\zeta - \eta s_d)^2 + 3\eta s_d(2\zeta + \eta s_d)\cos^2\alpha_0 \sin^2\theta] \tag{70}$$

where $\sigma_0 = \pi R^2$ is the geometrical cross section of the droplet and α_0 is the polarization angle, *i.e.*, the angle between he incident optical field the plane defined by **k** and $\mathbf{N}_d$. This equation shows the $1/\lambda^4$ dependence of the cross section, which is characteristic of the Rayleigh scattering. Averaging first over all orientations of the incident optical field to the plane **k**, $\mathbf{N}_d$ ($\langle \cos^2\alpha_0 \rangle = 1/2$) and then over all droplet director orientations gives finally the average sample cross section

$$\sigma^{\mathrm{RGA}} = \sigma_0 \frac{(2kR)^4}{108} [(\zeta - \eta s_d)^2 + \eta s_d(2\zeta + \eta s_d)(1 - s_E)] \tag{71}$$

The last equation gives the sample scattering cross section in terms of the droplet and the sample order parameters.

The second extreme case theoretically analyzed concerns the scattering from large *soft* droplets [18] where the condition

$$kR \gg 1 \tag{72}$$

is verified. For the visible light this condition holds for droplets larger than a few tenth of microns and settles a lower limit of approximately 0.1 μm to the droplet radius. Here, the anomalous diffraction approach (ADA) gives a better description than the RGA. The condition (72) allows the ray picture of the light propagation whereas the soft object approximation allow to neglect both the reflections on the external and internal boundaries and the refraction of the ray passing through the scattering object. Therefore, in the ADA approximation the droplet does not change either the direction of the propagation or the amplitude of the light wavefield but only introduces a phase shift which depends on the direction of the ray. The small differences between the directions of the field vectors **E** and **D** within the droplet as well as the slight between the ray direction and the wave vector, introduced by the anisotropic droplets, are also neglected. The approach which follows to calculate the far field distribution of the scattered light is very similar to the Fraunhofer diffraction pattern. Two contributions to the scattered light are considered: (a) the light scattered by a conjugated screen and (b) the light transmitted and phase shifted by the scattering droplet. Also in the ADA the theory gives a solution which can be expressed in a closed form only in the cases involving a complete alignment of the liquid crystal director inside the droplets (*i.e.*, in the case of high applied fields). In this case the droplets appear as uniformly aligned bodies with the liquid crystal direction **n** in each location parallel to the droplet director $\mathbf{N}_d$. In addition, to obtain detailed analytical results the further condition $kR < 5$ must be verified. Then, the total droplet scattering cross section is given by [18]

$$\sigma_d^{\mathrm{ADA}} = 2\sigma_0(kR)^2\left\{\cos^2\alpha_0\left[\frac{n(\theta)}{n_p} - 1\right]^2 + \sin^2\alpha_0\left[\frac{n_\perp}{n_p} - 1\right]^2\right\} \tag{73}$$

where n_p is the refraction index of the polymer matrix, n_0 and n_e are the ordinary and extraordinary indices of the liquid crystal, respectively, and

$$n(\theta) = \left[\frac{\cos^2\theta}{n_\perp^2} + \frac{\sin^2\theta}{n_\parallel^2}\right]^{-1/2} \tag{74}$$

It is possible to show that the same expression (73) of the droplet scattering cross section could be obtained in the RGA under the condition $kR > 1$. Therefore, Eq. (73) can be considered to be a good expression of the droplet scattering cross section in the case of well oriented droplets with radius R close to the boarder between the ADA and the RGA range of validity. We observe that many practical applications of PDLC materials involve these droplet sizes.

The condition $\Delta n = (n_{\parallel} - n_{\perp}) \ll n_{\perp}$ makes it possible to expand $n_e(\theta)$ as

$$n(\theta) = n_{\perp} + \Delta n \sin^2 \theta \tag{75}$$

and then (73) can be written as

$$\sigma_d = 2\sigma_0 (kR)^2 \left\{ \cos^2 \alpha_0 \left[\frac{(n_{\perp} + \Delta n \sin^2 \theta)}{n_p} - 1 \right]^2 + \sin^2 \alpha_0 \left[\frac{n_{\perp}}{n_p} - 1 \right]^2 \right\} \tag{76}$$

Averaging over the field and droplet director orientations as previously done gives the sample scattering cross section in terms of the sample order parameters s_E

$$\sigma = 2\sigma_0 (kR)^2 \left(\frac{\Delta n}{n_p} \right)^2 \left[\left(\frac{\delta}{\Delta n} \right)^2 - \frac{2}{3} \frac{\delta}{\Delta n} (1 + s_E) + \frac{4}{105} (7 - 10 s_E + 3\langle P_4 \rangle) \right] \tag{77}$$

where P_4 is the fourth order Legendre polynomial of the sample and $\delta = n_p - n_{\perp}$ is a measure of the mismatch between the refraction index of the polymer and the ordinary refractive index of the liquid crystal. Eq. (77) indicates a quadratic dependence on the wavenumber and also a quadratic dependence of the index mismatch Δn. If $\delta = 0$, the scattering cross section σ is a monotonically decreasing function of s_E which vanishes when the droplets are parallel to the applied field.

The transmitted intensity *vs.* applied voltage (I, V) characteristic curve of the PDLC is obtained by inserting Eq. (77) into (56), which gives $I = I(s_E)$, and the computing $s_E(V)$ to obtain finally $I(V)$. A

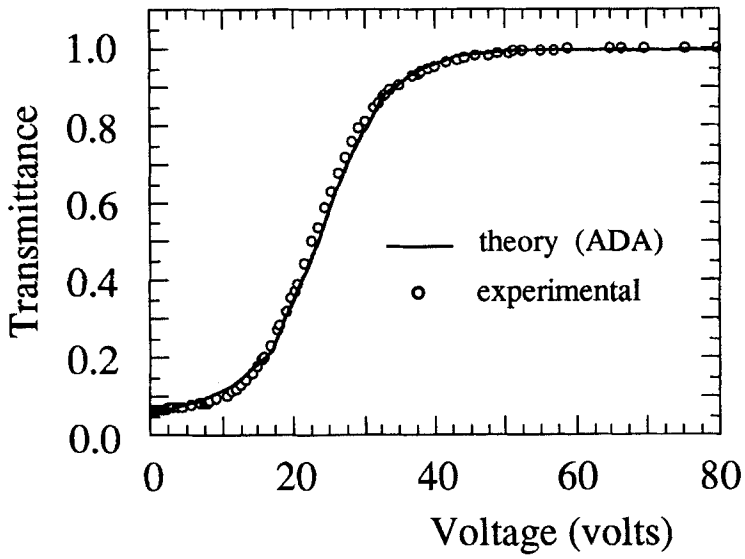

FIGURE 8 Optical transmittance of a 23-μm thick PMMA/E7 PDLC film (prepared by the PIPS method) as function of the applied voltage in the anomalous diffraction regime.

satisfactory fit of the experimental data can be obtained using this method as shown in Figure 8.

4. OPTICAL PHASE RETARDATION

4.1. Optical Phase Shift

The analysis of the optical phase shift in PDLC is interesting because this phenomenon is strictly related to both the droplet reorientation and the liquid crystal reorientation inside the droplets. The calculation of the optical phase shift induced by a polymer-dispersed liquid crystal when subjected to a low frequency electric field requires first working out the ordinary and extraordinary refractive indices of the droplet and their dependence on the droplet's order parameter. This has be first done by Basile *et al.* [23] who reported a detailed study of the optical phase shift induced by a PDLC sample subjected to a low frequency electric field. Within this model, a small liquid crystal

volume of the droplet with a uniform orientation given by the local director $\mathbf{n}(\mathbf{r})$ is first considered. Figure 9 shows the local-index ellipsoid corresponding to this volume, whose principal axes are $n_{\parallel}$ and $n_{\perp}$ ($n_{\parallel}$ and $n_{\perp}$ are the liquid crystal refractive indices). In this figure the droplet director $\mathbf{N}_d$ is chosen parallel to $\mathbf{n}_z$; accordingly, the wave with wavevector $\mathbf{k}_1$ and electric displacement D_1 is affected by the ordinary index of the droplet, while the wave with wavevector $\mathbf{k}_2$ and electric displacement D_2 experiences the extraordinary index.

The extraordinary index of the whole droplet is defined as the average index experienced by a light wave travelling in a direction perpendicular to $\mathbf{N}_d$ and with polarization parallel to it. The local refractive index $n_e(\mathbf{r})$ experienced by such wave in the small volume of liquid crystal considered depends on the angle ψ between $\mathbf{n}(\mathbf{r})$ and the

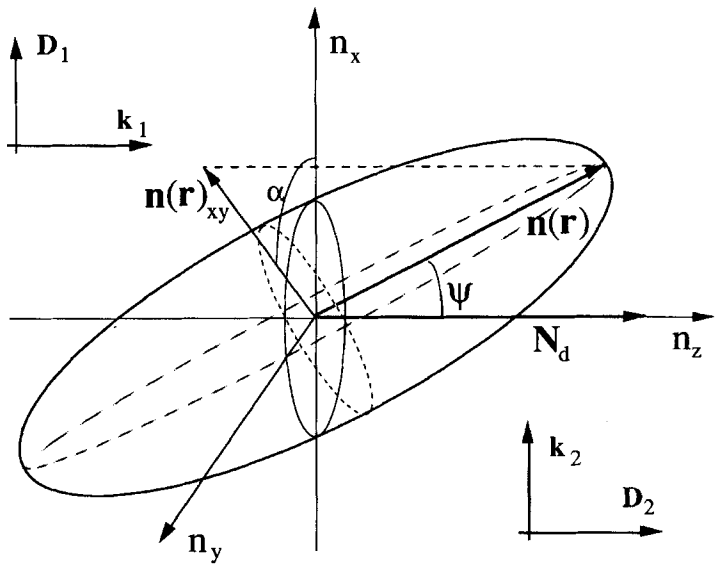

FIGURE 9 Local-index ellipsoid corresponding to a small volume of the liquid crystal inside a droplet ($\mathbf{n}_x$, $\mathbf{n}_y$ and $\mathbf{n}_z$ are the unit vectors of the coordinate axes x, y and z, respectively). The full line ellipse represents the intersection of the ellipsoid with the plane ($\mathbf{n}_x$, $\mathbf{n}_y$). The droplet director $\mathbf{N}_d$ lies along $\mathbf{n}_z$ and $\mathbf{n}(\mathbf{r})_{xy}$ is the projection $\mathbf{N}_d$ of over the plane ($\mathbf{n}_x$, $\mathbf{n}_y$). ψ is the angle between $\mathbf{n}(\mathbf{r})$ and $\mathbf{N}_d$. The wave with wavevector $\mathbf{k}_1$ is affected by the ordinary index of the droplet whereas the wave with wavevector $\mathbf{k}_2$ experiences the extraordinary index.

polarization direction as

$$n_e(\mathbf{r}) = \frac{n_{\parallel} n_{\perp}}{[n_{\parallel}^2 \sin_{\psi}^2 + n_{\perp}^2 \cos^2 \psi]^{1/2}} \tag{78}$$

The last equation is simply obtained by considering the intersection of the ellipsoid with a plane parallel to the incident wavefront, which gives an ellipse with axes $n_{\perp}$ and n where $n_{\perp} < n < n_{\parallel}$, and then intersecting this ellipse with the polarization direction.

The extraordinary refractive index of the droplet n_{ed} is then obtained by averaging $n_e(\mathbf{r})$ over all director orientations within the droplet volume

$$n_{\text{ed}} = \langle n_e(\mathbf{r}) \rangle_{V_d} = \int n_e(\mathbf{r}) f(\mathbf{r}, \psi, \alpha) r^2 \sin \psi \, dr d\psi d\alpha \tag{79}$$

where $f(\mathbf{r}, \psi, \alpha)$ is the distribution function of the liquid crystal director inside the droplet, which depends on the droplet's shape, the anchoring at the boundaries and the external applied fields. In the case of small droplets the bipolar configuration, which possess cylindrical symmetry around $\mathbf{N}_d$, is the most probable one and we will limit the following discussion to this case. The dependence of the distribution function f on the angle ψ can be described very easily if an approximation is introduced which consists in replacing the actual director configuration with a simpler equivalent one, *i.e.*, a simpler configuration which produces the same value of the droplet' order parameter s_d. As shown in Ref. [23], this approximation introduces in the calculation of the optical phase shift an error which is very small (of the order of 1% or even lower). Accordingly, after defining an average angle ψ_{av} such that

$$\cos^2 \psi_{\text{av}} = \langle \cos^2 \psi \rangle_{v_d} = \frac{1}{3}(2s_d + 1) \tag{80}$$

we can consider a uniform distribution where $\psi = \psi_{\text{av}}$

$$f(\mathbf{r}, \psi, \alpha) = f(\psi) = \frac{3}{2} \frac{\delta(\psi - \psi_{\text{av}})}{\pi R_{\text{eff}}^3 \sin \psi_{\text{av}}} \tag{81}$$

where $\delta(\psi - \psi_{\text{av}})$ is the Dirac function and the other constants are required by the normalization condition (considering spherical droplets

with an effective radius R_{eff})

$$\int_0^{R_{\text{eff}}} \int_0^{\pi/2} \int_0^{2\pi} f(\mathbf{r}, \psi, \alpha) r^2 \sin\psi \, dr d\psi d\alpha = 1 \tag{82}$$

With f expressed in the form of Eq. (82), the integration is straightforward and gives

$$n_{\text{ed}}(s_d) = \frac{n_{\parallel} n_{\perp}}{\left[n_{\parallel}^2 + \frac{1}{3}(n_{\perp}^2 - n_{\parallel}^2)(2s_d + 1)\right]^{1/2}} \tag{83}$$

where the definition (80) has been used. A similar calculation gives the ordinary refractive index of the droplet, which is defined as the average index experienced by a light wave travelling in a direction parallel to $\mathbf{N}_d$ and with any polarization lying in a transverse plane. In this case, the local ordinary index depends on the polarization angle α (see Fig. 10)

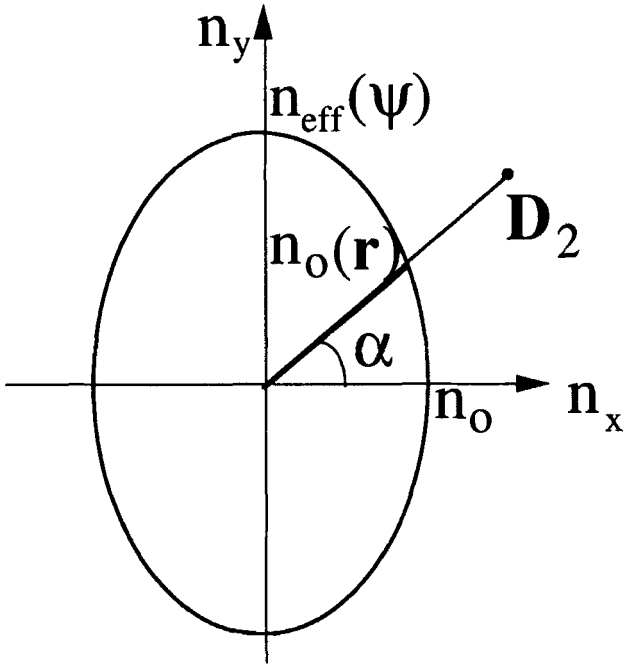

FIGURE 10 The ellipse obtained by intersecting the local index ellipsoid with the plane xy normal to the droplet director $\mathbf{N}_d$ (see also Fig. 9). The local ordinary index $\mathbf{n}_0(\mathbf{r})$ is given by the intersection of this ellipse with the polarization direction.

and varies from the maximum value $n(\psi)$ (for $\alpha = 0$) to the minimum value n_0 (for $\alpha = \pi/2$).

The average droplet index is then calculated as

$$n_{od} = \int_0^{R_{eff}} \int_0^{x/2} f(\psi) r^2 \sin\psi \, dr d\psi \int_0^{2\pi} n_0(\mathbf{r}) d\alpha \tag{84}$$

Following the calculations reported in Ref. [23], it is finally found

$$n_{od}(s_d) \approx \frac{2}{\pi} n_0 F\left(\frac{\pi}{2}, m(s_d)\right) \tag{85}$$

where

$$m(\psi) = \frac{\sqrt{n^2(\psi) - n_\perp^2}}{n(\psi)} \tag{86}$$

and $F(\pi/2, m(\psi))$ is the complete elliptical integral of the first kind defined by

$$F\left(\frac{\pi}{2}, m\right) = \int_0^1 \frac{dx}{[(1-x^2)(1-m^2x^2)]^{1/2}} \tag{87}$$

Figure 11 reports the trend of n_{ed} and n_{od}, calculated by means of Eqs. (84) and (86), respectively, *versus* the droplet's order parameter s_d for bipolar droplets of nematic of the liquid crystal E7. We observe that as s_d approaches the unitary value, which corresponds to a perfect alignment of the liquid crystal director along the droplet axis, n_{ed} and n_{od} approach the value n_0 and n_e, respectively. When s_d approaches zero, *i.e.*, the configuration of the liquid crystal inside the droplet tends to a random orientation, both n_{ed} and n_{od} approach the refractive index $n_{iso} = (n_\parallel + 2n_\perp)/3$ of an isotropic droplet.

The model described has been successfully applied to study the optical phase shift induced by a PDLC sample. We observe that, besides the theoretical interest, the determination of the optical phase shift has also a practical important because it can be used as a probe of the droplet realignment. We start by considering the contribution of a single droplet. Referring to Figure 12, the light polarization is described by the vector **D** in the xy plane and ψ_d and η_d are the Euler angles

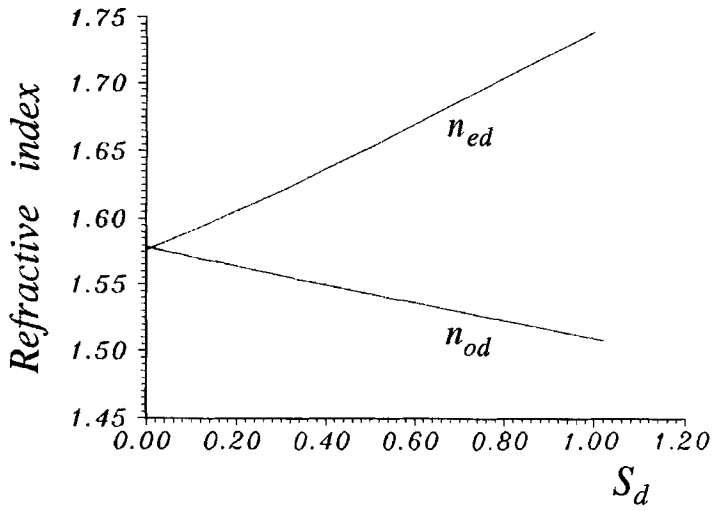

FIGURE 11 The ordinary and extraordinary refractive indexes of a nematic droplet *vs.* its order parameter s_d (after Ref. [23]).

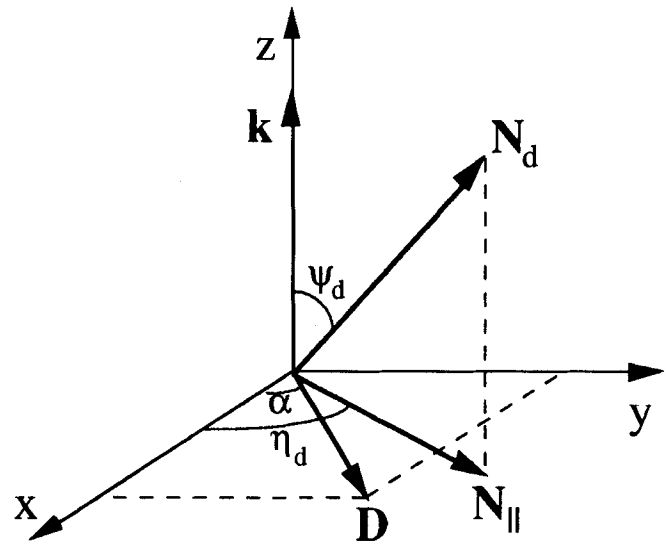

FIGURE 12 Reference frame used for the evaluation of the optical phase shift experienced by a monochromatic plane wave (propagating along the z axis) when it crosses a nematic droplet.

determining the orientation of $\mathbf{N}_d$ in the laboratory frame x, y, z when the wavevector $\mathbf{k}$ is parallel to z.

The two components of $\mathbf{D}$, parallel and perpendicular to $\mathbf{N}_d$, are

$$\begin{aligned} \mathbf{D}_\perp &= \mathbf{D}\sin(\eta_d - \alpha) \\ \mathbf{D}_\parallel &= \mathbf{D}\cos(\eta_d - \alpha) \end{aligned} \tag{88}$$

respectively, where α is angle of the polarization axis with respect to the x axis (see Fig. 12). Inside the droplet the two components $\mathbf{D}_\perp$ and $\mathbf{D}_\parallel$ experience the refractive index n_{od} and n_d^{eff}, respectively, where

$$n_d^{\text{eff}} = \frac{n_{\text{od}} n_{\text{ed}}}{[n_{\text{od}}^2 \sin^2\psi_d + n_{\text{ed}}^2 \cos^2\psi_d]^{1/2}} \tag{89}$$

so that, after travelling through one droplet, they will be phase shifted by the angle

$$\phi^*(s_d;\psi_d) = \frac{2\pi}{\lambda}\langle d\rangle_{V_d}[n_d^{\text{eff}} - n_{\text{od}}] \tag{90}$$

where $\langle d\rangle_{V_d}$ is the average path inside the droplet. Since for a spherical cavity with radius R it is $\langle d\rangle_{V_d} = (4/3)R$, we obtain

$$\phi^*(s_d;\psi_d) = \frac{8\pi}{3\lambda}R\left[\frac{n_{\text{od}}(s_d)n_{\text{ed}}(s_d)}{[n_{\text{od}}^2(s_d)\sin^2\psi_d + n_{\text{ed}}^2(s_d)\cos^2\psi_d]^{1/2}} - n_{\text{od}}(s_d)\right] \tag{91}$$

Accordingly, after crossing one droplet and in the local frame of the droplet we have

$$\begin{aligned} \mathbf{D}_\perp(t) &= \mathbf{D}_\perp\cos(\omega t) \\ \mathbf{D}_\parallel(t) &= \mathbf{D}_\parallel\cos(\omega t + \phi^*) \end{aligned} \tag{92}$$

These equations can be finally transformed into the laboratory frame to give

$$\begin{aligned} \mathbf{D}_x(t) &= a\cos(\omega t + \delta_x) \\ \mathbf{D}_y(t) &= b\cos(\omega t + \delta_y) \end{aligned} \tag{93}$$

where a, b and the phase angles δ_x and δ_y are defined in terms of $\mathrm{D}_\perp$, $\mathrm{D}_\parallel$, η_d and ϕ^*.

The phase shift induced by single droplet is given by the difference $\delta_y - \delta_x$ which can be expressed as a function of the liquid crystal's orientation inside the droplet (s_d), the polarization angle (α) and the droplet orientation (ψ_d and η_d), *i.e.*,

$$\phi_d(\alpha, s_d; \psi_d, \eta_d) = \delta_y - \delta_x \tag{94}$$

In the absence of external electric fields, the phase shift introduced by the whole sample is zero since the random orientation of the droplets does not produce any net average phase shift. When an electric field **E** is applied, the droplet directors try to orient along the field direction and, except the case in which the propagation direction of the incident beam coincides with the direction of the electric field, such reorientation produces a non-zero net phase shift. To correlate such phase shift to the droplets orientation we proceed as follows. We consider first a layer of the PDLC sample which is enough thin such that the incident light beam (whose cross section is supposed to be much larger than the droplet size) crosses at most one droplet's layer. The optical phase shift associated to such a thin film of the PDLC can be calculated by averaging over all possible orientations of the droplets which depend on the applied field As previously done in the calculation of n_{ed}, we replace the actual distribution of the droplet directors $\mathbf{N}_d$ around the field direction with the simplest equivalent distribution, *i.e.*, witht he simplest distribution which gives the same value of the order parameter s_E. Accordingly, we use the following normalized distribution function

$$f(\gamma) = \frac{1}{2} \frac{\delta[\gamma - \gamma_{av}(E)]}{\pi \sin \gamma_{av}(E)} \tag{95}$$

where γ_{av} is the average angle γ between $\mathbf{N}_d$ and **E** defined by

$$\cos^2 \gamma_{av} = \langle \cos^2 \gamma \rangle_{V_d} = \frac{1}{3}[2s_E + 1] \tag{96}$$

It is then easy to work out the phase shift ϕ_1^* induced by the considered single droplet layer. In fact, in the local frame $x'y'z'$ shown in Figure 13, it is

$$\phi_1^* = \int_0^{2\pi} \int_0^{\pi/2} \phi_d(\gamma, \xi) f(\gamma) d\gamma d\xi \tag{97}$$

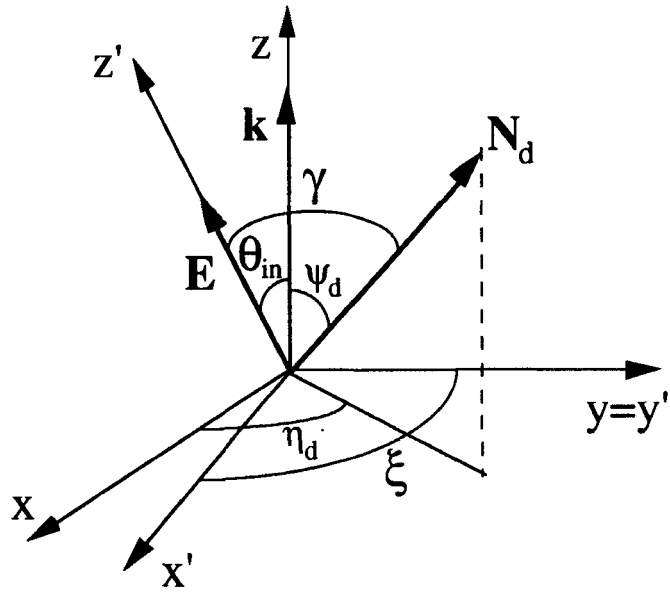

FIGURE 13 Relation between the reference frame xyz (described in Fig. 12) and the local reference frame $x'y'z'$ introduced to evaluate the optical phase shift. θ_{in} is the angle between the incident light and the applied field.

where $\phi_d(\gamma, \xi)$ is given by Eq. (94) once transformed to the local frame and the angles γ and ξ related to η_d and ψ_d through the angle θ_{in} between the incident light wavevector and the applied field (which usually is normal to the boundary walls of the sample).

The integration in Eq. (97) can be performed by numerical methods and the result will be dependent on α, θ_{in}, s_d and the applied field through s_E, *i.e.*,

$$\phi_1^* = \phi_1^*[\alpha, \theta_{in}, s_d, s_E] \tag{98}$$

To find the contribution of the whole sample to the phase shift we need to evaluate the number N_l of single elementary droplet layers crossed by the incident beam. If the case of a uniform droplet distribution in the isotropic polymeric matrix, the volume fraction v_{lc} of the liquid crystal gives also the fraction of the total optical path of the radiation through the droplets. Then, the thickness of the elementary layer is

given by

$$d^*(\theta_{in}) = (1/v_{1c})d_{eff}\cos\theta_{in} \tag{99}$$

where $d_{eff} = (4/3)R_{eff}$ is the effective optical path in one droplet, and the number of layers is simply

$$N_1 = \frac{dv_{1c}}{d_{eff}\cos\theta_{in}} \tag{100}$$

Finally, the overall optical phase shift introduced by the sample is

$$\Delta\phi = N_1\phi_1^* = \phi_1^*[\alpha, \theta_{in}, s_d, s_E] \tag{101}$$

Figure 14 shows the dependence of $\Delta\phi$ on the applied voltage V for different values of θ_{in} and assuming $d = 36\,\mu m$, $R_{eff} = 150\,nm$ and $\zeta = 0.16$. Figures 15 and 16 show the influence of the materials parameters R_{eff} and ζ, respectively, on the characteristic $\Delta\phi$ *vs.* V (assuming $\theta_{in} = 20°$). We observe that both ζ and R_{eff} strongly affect the droplet reorientation and, consequently, the slope of the phase shift curve

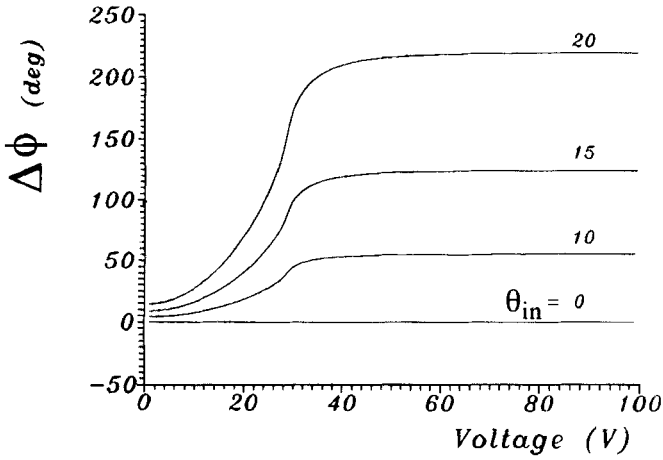

FIGURE 14 The theoretical behavior of the optical phase shift $\Delta\phi$ as function of the applied voltage at different values of θ_{in}. The thickness of the PDLC film is assumed $d = 36\,\mu m$ and the values used for the parameters R_{eff} and ζ are 150 nm and 0.16, respectively (after Ref. [23]).

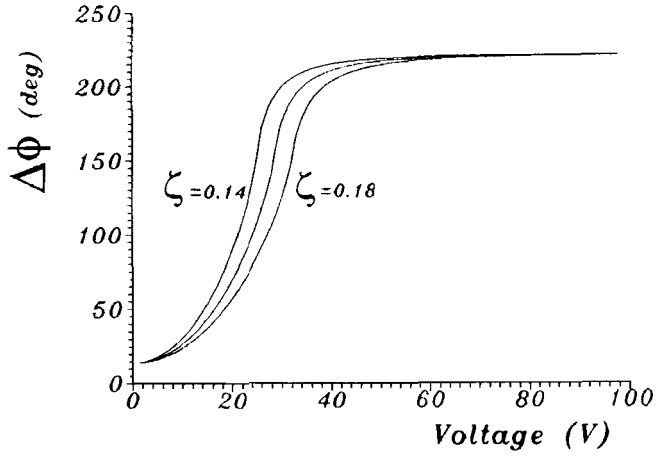

FIGURE 15 The theoretical behavior of the optical phase shift $\Delta\phi$ as function of the applied voltage at different values of R_{eff}. The thickness of the PDLC film is assumed $d = 36\,\mu\text{m}$ and the values used for the parameters θ_{in} and ζ are 20° and 0.16, respectively (after Ref. [23]).

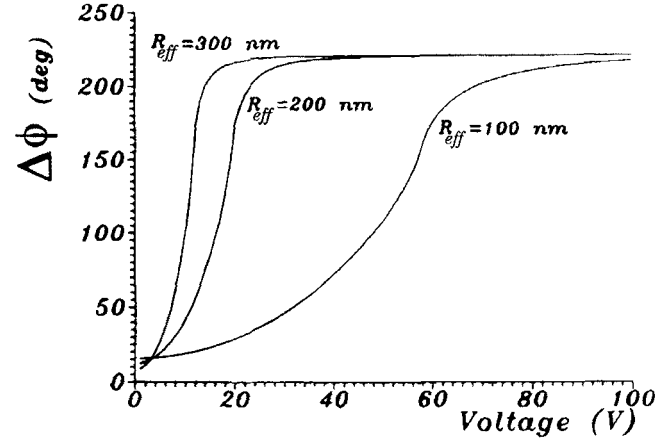

FIGURE 16 The theoretical behavior of the optical phase shift $\Delta\phi$ as function of the applied voltage at different values of ζ. The thickness of the PDLC film is assumed $d = 36\,\mu\text{m}$ and the values used for the parameters θ_{in} and R_{eff} are 20° and 150 nm, respectively (after Ref. [23]).

from the low field region up to the saturation. In these simulations s_d is considered to be independent on the applied field. However, as shown by the comparison with experimental data obtained by a conventional

ellipsometric technique [23], a better agreement between theory and experiment is obtained if the droplet order parameter s_d is assumed to be field-dependent. This assumption seems to be quite reasonable since we expect that not only the field director is aligned by the applied field but also that the orientation of the average liquid crystal director of the droplet axis is affected by it.

In Figure 17 we report a comparison between the $\Delta\phi$ *vs* V experimental curves obtained for different values of the incidence angle θ_{in} and the theoretical curves calculated by assuming the following empirical equation to express the dependence of s_d on the applied voltage

$$s_d = 1 - \frac{V_c(1 - s_d^m)}{V_c + (1 - s_d^m)V} \tag{102}$$

where V_c and s_m^d are the fit parameters. The experimental data have been fitted using $s_d^m = 0.7$ and $V_c = 10\,\text{V}$. The result is remarkable since for the different values of θ_{in} a satisfactory agreement is obtained using the same values of the parameters ζ and R_{eff}.

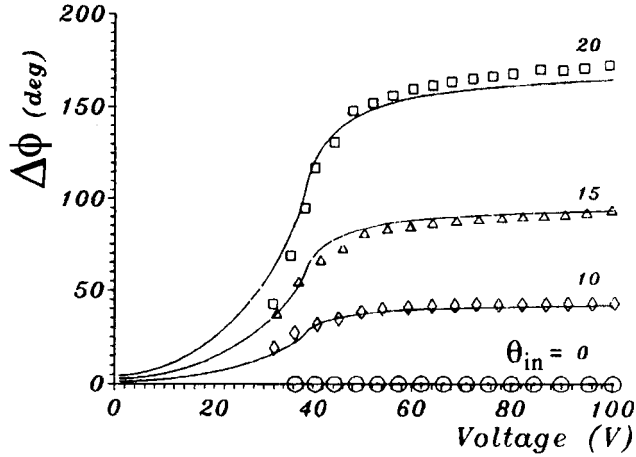

FIGURE 17 The measured optical phase shift *vs.* applied voltage for different values of θ_{in}. The symbols are the experimental values; the full lines represent the theoretical results corrected according to Eq. (104) (after Ref. [23]).

4.2. Thermal Effects

The electrooptical properties of PDLC are strongly affected by the temperature. This is essentially due to the liquid crystal since its physical properties are very sensitive to the thermal conditions. Even though the temperature is a very important parameter to be considered even for practical applications, a systematic study of the temperature effects has not yet been performed up to now and the data reported in the literature concern essentially the temperature dependence of the transmission characteristics [24] and of the optical phase shift [25].

A first consequence of this temperature dependence is that it is possible to induce the switching from the opaque to the transparent state by simply increasing the temperature of the PDLC sample. In fact, the refractive index of the polymer binder is usually close to both the ordinary refractive index and the isotropic refractive index of the liquid crystal. Thus, if the temperature of the sample is raised above the transition temperature to the isotropic state of the liquid crystal, a satisfactory index matching is usually found between the droplets and the polymeric matrix, even if such effect is not as good as in the case of the application of an external voltage. Actually, the refractive indexes of the liquid crystal are temperature dependent so that a slight variation of the transmission properties is already observed close to the transition temperature before reaching the isotropic state.

This effect is the basis of several experiments involving nonlinear optical phenomena as described in following paper in this volume.

The experimental data reported in the literature on the transmission characteristics of PDLC indicate a reduction of the threshold voltage for reorientation with increasing temperature. This behavior can be qualitatively explained by considering the dependence of the threshold voltage on the material parameter K, g and $\Delta\varepsilon$, expressed in Eq. (40). In fact, if we assume to a first approximation a similar thermal behavior for the conductivities σ_d and σ_p, the factor which dominates the temperature dependence of the threshold voltage is the ratio $K/g\Delta\varepsilon$. This latter is proportional to the scalar order parameter s which is a decreasing function of the temperature. A more detailed analysis of the phenomenon has been performed by studying the temperature dependence of the optical phase shift [25]. The results indicate that it is possible to relate the threshold voltage to an *effective elastic constant*

K_d defined as

$$K_d = K\left(\frac{\zeta}{R_{\text{eff}}}\right)^2 \tag{103}$$

which combines the elastic properties of the liquid crystal droplet, through the constant K, ad the shape effects, through ζ and R_{eff}. The experimental data indicted that the quantity K_d is a decreasing function of the temperature.

An example of the behavior of the optical phase shift with the temperature is shown in Figure 18.

The temperature dependence of the switch-on time τ_{ON} has also been investigated [26] as it is an important aspect characterizing the performance of a PDLC sample. It was found that the reduction of the viscosity with increasing the temperature is the effect which dominates the dependence of τ_{ON} on the temperature. Figure 19 shows the behavior of the switch-on time with the intensity I_0 of the incident light, measured on a PDLC doped with a dye in order to enhance the thermooptical response. The observed reduction of τ_{ON} with increasing I_0 is easily explained by Eq. (44) considering that higher intensity is equivalent to higher temperature of the sample spot crossed by the beam, and hence lower viscosity.

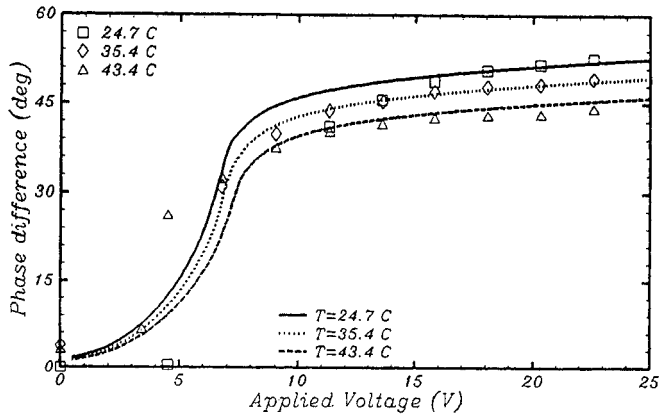

FIGURE 18 The behavior of the optical phase shift *vs.* applied voltage at different temperature (after Ref. [25]).

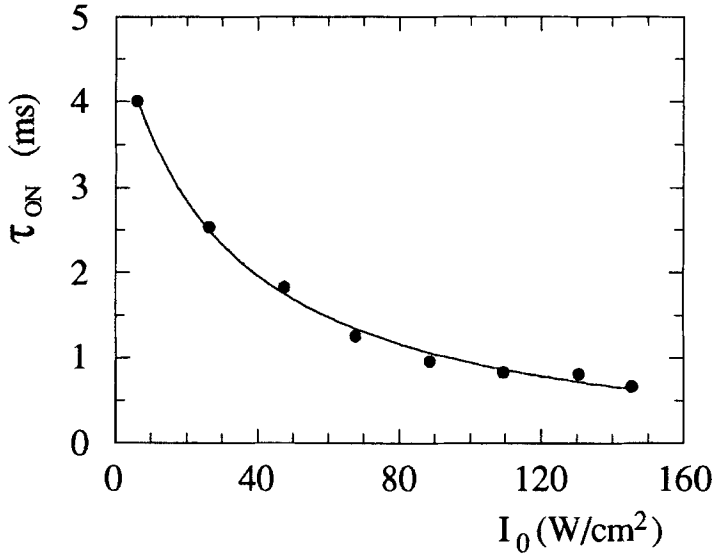

FIGURE 19 The switch-on time constant τ_{ON} on the linear transmission of a PDLC sample *vs.* the intensity I_0 of the incident light beam. A low frequency square voltage of 50 V is applied to the sample.

5. NONLINEAR OPTICAL PROPERTIES

5.1. Preliminary Considerations

The interest in the study of the nonlinear optical properties of materials has enormously grown in the last few years. In fact, while these properties provide new methods for the investigation of physical phenomena, at the same time they offer the possibility of several new technology applications.

It is known that any material has a nonlinear optical behavior associated with the perturbation either of the electronic wavefunctions or of the molecular orientation. This behavior can be described by means of a dielectric polarization **P** written as a series expansion of the electric field [27].

$$\mathbf{P} = \underline{\chi}^{(1)}\mathbf{E} + \underline{\chi}^{(2)}\mathbf{EE} + \underline{\chi}^{(3)}\mathbf{EEE} + \cdots \tag{104}$$

where $\underline{\chi}^{(i)}$ are the dielectric susceptibility tensors. The first term gives the conventional response of the medium to the incident field while the higher order terms describe the nonlinear behavior. Typical values of the second-order susceptibility term $\chi^{(2)}_{ijk}$ for materials in the condensed state are $10^{-8}-10^{-9}$ esu whereas the third-order susceptibility terms $\chi^{(3)}_{ijkl}$ typically range between 10^{-11} and 10^{-15}esu, which are very small compared to $\chi^{(1)}_{ij} \approx 0.1$ Eq. (104) greatly simplifies when the symmetry properties of the medium are considered and when specific field polarizations are assumed. In particular, in the case of centrosymmetric media, all the terms of $\underline{\chi}^{(n)}$ with n even are zero [28] and the even order nonlinearities disappear. In these media (as for instance gases, isotropic liquid and cubic crystal) second order nonlinear effects such as second armonic generation can not be produced and the first nonlinear response is given by $\underline{\chi}^{(3)}$. This is also the case for liquid crystal most of the time.

If a linearly polarized monochromatic optical wave is considered to propagate through a centrosymmetric medium, the nonlinearity produces a change of the dielectric permittivity proportional to the light field intensity, *i.e.*,

$$\underline{\varepsilon} = \underline{\varepsilon}_0 + \frac{1}{2}\underline{\varepsilon}_2 |\mathbf{E}|^2 \tag{105}$$

where $\underline{\varepsilon}_0$ is the usual linear response and $\underline{\varepsilon}_2 = 8\pi\underline{\chi}^{(3)}$. Usually in condensed media the terms of $\underline{\varepsilon}_2$ are very small, being of the order of $10^{-10}-10^{-14}$esu. In liquid crystals, however, the collective reorientation properties produced by the long-range orientation order of the molecules give rise to a peculiar nonlinear behavior so that values of ε_2 of the order of 0.1 esu can be easily reached. This extraordinary large nonlinear optical response, also called *giant optical nonlinearity* (GON), was discovered in 1980 [29] and since that time was studied by many scientists [30, 31]. It has been demonstrated that the optically induced reorientation of the liquid crystal director is responsible for such effect.

A second phenomenon which assumes peculiar features in liquid crystals is the so-called thermal indexing. It consists of a change of the refractive indexes of the material as a consequence of the heating caused by a partial absorption of the incident light. This effect gives rise to a nonlinear response of the medium whose refractive index becomes dependent on the light intensity. This kind of nonlinearity is

particularly interesting in liquid crystals because the thermal gradients of the refractive indexes are about two order of magnitudes larger than they are in usual nonlinear liguids and have a critical behavior close to the phase transitions.

While the nonlinear optical effects concerning the nematic liquid crystals in the usual configurations is a subject which has widely grown in the recent years and has now a number of well established basic ideas [14], the nonlinearity in PDLC is a very new field of research which has yet mostly to be investigated (the first optical nonlinearity of PDLC has been reported in 1989 [32]). In addition, even if the nonlinear phenomena are a consequence of the nonlinear properties of the liquid crystal, the confined geometry of the liquid crystal in PDLC gives some peculiarities to the nonlinear response of these materials. As a consequence, the content of following sections must simply be considered as a report of recent achievements which are not complete and deserve further detailed studies.

5.2. Self-transparency

Self-transparency due to thermal nonlinearities is a basic effect in PDLC. It has consequences on the wave mixing process, leading to optooptical switch and self-diffraction with threshold. This effect consists in the switching of a PDLC sample from the opaque (OFF) state to the transparent (ON) one driven by the sample heating produced by the incident laser beam.

The experimental observation of such effect represented the first direct evidence of a strong optical nonlinearly induced by a laser field in a PDLC sample [32]. A schematic picture of the experimental set-up used is shown in Figure 20.

A typical experimental result is shown in Figure 21 where the transmission t, *i.e.*, the ratio between the transmitted optical power p_f and the incident one P_i, is plotted *vs.* P_i. A clear switching effect is observed (with a threshold at about 50 mW) which is completely reversible as for the case of the electrically induced switching. The thermal origin of the effect was confirmed by time response measurements performed by chopping the incident laser beam at low frequency [32], a rise time of the detected signal of about 20 ms was measured, which is in the typical range of thermal effects in liquid crystals.

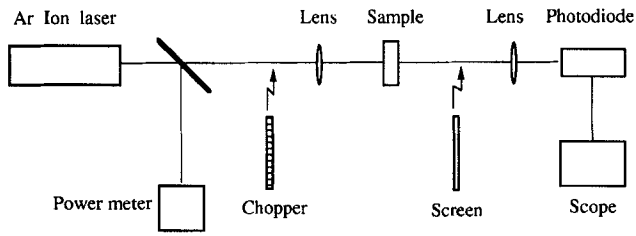

FIGURE 20 Schematic representation of the experimental set-up used to study optical nonlinearities induced by thermal effects in PDLC. The light beam from an argon ion laser (λ = 5145 Å) is focused on the sample at normal incidence; the transmitted optical power is detected by a photodiode. A beam splitter placed before the sample enables one to measure the impinging optical power.

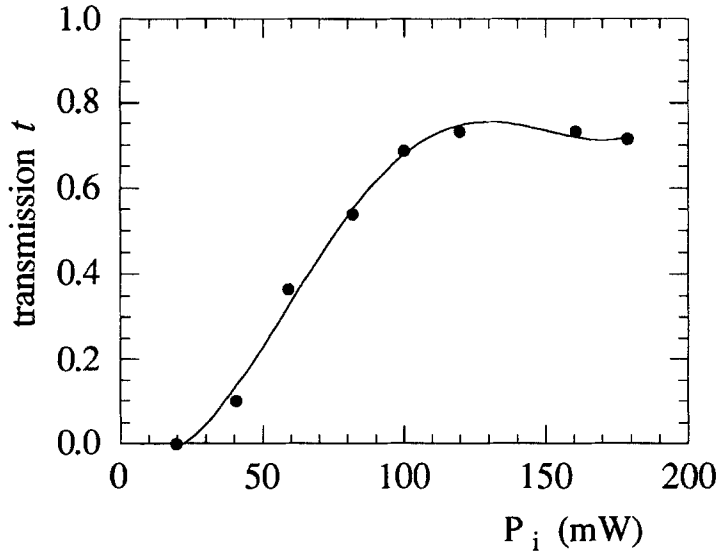

FIGURE 21 Typical behavior of the transmission t as function of the incident power. The PDLC sample used in this experiment was prepared by the PIPS method using the nematic liquid crystal E7 with the addition of 0.1% of an absorbing dye to enhance the thermal response.

Self-transparency was observed for the first time in a composite material consisting of fused quartz particles dispersed in a liquid mixture [34], however, up to now, no material exhibited contrast ratios between the ON and OFF states better than those obtained with

PDLC. The quenching of the scattering due to the nonlinear response of a given medium consisting of inclusions randomly distributed into a different material (like nematic droplets into the polymeric binder) can be explained considering that the amount of scattered radiation depends, in the weak scattering limit, on the square of the difference Δn of the refractive indexes, $n_d = n_{0d} + \delta n_d$ (I) and $n_p = n_{op} + \delta n_p$ (I), of the two media

$$\Delta n = (n_{0d} - n_{0p}) + (\delta n_d(I) - \delta n_p(I)) = \Delta n^0 + \Delta n^{\mathrm{NL}}(I) \tag{106}$$

where n_0 and δ_n are the linear and nonlinear parts, respectively, and I is the intensity of the laser radiation. Thus, the scattering coefficient is expressed as

$$s = g(\Delta n)^2 \tag{107}$$

where g is a constant dependent on size, shape, density and other feature of the inclusions. If Δn^0 and $\Delta n^{\mathrm{NL}}(I)$ have opposite signs and $|\Delta n^{\mathrm{NL}}(I)|$ increases with the intensity I, Δn becomes smaller with increasing I and at a certain $I = I_{\mathrm{th}}$ the condition

$$\Delta n^{\mathrm{NL}}(I_{\mathrm{th}}) = -\Delta n^0 \tag{108}$$

may be reached thus making $s = 0$. At $I = I_{\mathrm{th}}$ the scattered light drops to zero with the consequent rise of transmission; we speak then of self-transparency of the nonlinear material since transparency has been reached by increasing the intensity. In PDLC samples, the phenomenon can be explained as follows. The light impinging on the sample is partially absorbed and this results in an increase of the temperature of the liquid crystal droplets. The induced change of the droplet effective refractive index is small and has a little influence on the scattering coefficient until, after increasing the intensity above a certain threshold the temperature T_c of the transition to the isotropic phase is reached. Thus, the scattering coefficient approaches zero depending on the fulfilment of the index matching condition $\Delta n = 0$. Since in PDLC the nonlinearity of the matrix can typically be neglected with respect to the one of the droplet one has

$$\Delta n = \Delta n^0 + \delta n_{\mathrm{d}}(I) \tag{109}$$

The effective refractive index n_{0d} of a droplet is a mixture of the extraordinary and ordinary refractive indexes of the liquid crystal, n_e and n_0, and is typically quite different from n_{0p} ($\Delta n^0 \sim 0.1$). This is the reason why strong light scattering occurs below the threshold. When the temperature of the sample increases approaching T_c we expect dn_{0d}/dT to be slightly negative, since $dn_e/dT < 0$, $dn_o/dT > 0$ and $|dn_e/dT| > |dn_o/dT|$, but a big jump to a smaller value $n_i < n_{0d}$ occurs at the phase transition where $\Delta n^0 = 0.01 / 0.02$. For thermal effects it is $\delta n_d(I) < 0$ and thus the nonlinear contribution can counterbalance the small index mismatch Δn^0 and produce self-transparency.

The consideration reported above provide a qualitative explanation of the phenomenon. A detailed description of the transmission *vs.* impinging intensity characteristic must take into account the Gaussian intensity distribution $I(r)$ of the light beam

$$I(r) = I_0 e^{-(r^2/w^2)} \tag{110}$$

which is supposed to produce a Gaussian temperature distribution $T(r)$ over the sample

$$T(r) = T_r + \delta T_0 e^{-(r^2/r_0^2)} \tag{111}$$

where r is the distance from the axis of the beam, w is the spot size and δT_0 is the on-axis temperature rise assumed proportional to the absorbed power. Such temperature distribution induces self-transparency in the centre of the beam before than in the tails. The theoretical calculation of the transmission characteristic has been performed [14, 35] under the assumptions of (*i*) a transient regime for the temperature distribution (which allows to set $r_0 = w$ in Eq. (111) and (*ii*) a proportionality relation between the absorbed power and the incident one. The result for the overall transmittivity t of the sample through the beam cross section is

$$t(P_i) = t_i + (t_n - t_i)\frac{P_{\text{th}}}{P_i} \tag{112}$$

where t_i and t_n are the transmission of the sample corresponding to the isotropic state and the mesomorphic (nematic) state of the droplets, respectively, and P_{th} is the threshold power, *i.e.*, the value of the

impinging power corresponding to an on-axis temperature equal to Tc. Since in PDLCs it is $t_n \ll t_i$, Eq. (112) reduces to

$$\begin{aligned} t(\mathbf{P}_i) &\approx t_i \left[1 - \frac{P_{\text{th}}}{P_i}\right] \quad \text{for } P_i > P_{\text{th}} \\ t(\mathbf{P}_i) &\approx 0 \qquad \text{for } P_i < P_{\text{th}} \end{aligned} \tag{113}$$

Calculations based upon this approach allow to give satisfactory description of the experimental data under the transient regime conditions [35]. The good agreement of the theory with the experimental data shows that this simple model for the formation of an area of isotropic droplets in the sample gives a satisfactory explanation of the smooth switching in self-transparency.

An effect somehow opposite to self-transpareny, consisting in an optical power limiting, was observed by Palffy-Muhoray [36, 2] on the same kind of PDLC (prepard by PIPS method). In this experiment an a.c. voltage (1 KHz) was applied to the sample in order to keep it in the transparent state and the transmittivity was probed by a weak He-Ne laser beam while an Argon laser was used as pump beam. A considerable lowering of the transmittivity (from 0.8 to 0.3) was measured changing the temperature with no pump excitation. A similar behavior was observed keeping the sample at a constant temperature and increasing the intensity of the pump. these experimental results can be explained considering that while index matching is initially redalized in the sample by the electric field induced alignment, the following heating of the sample through the phase transition temperture produces isotropic droplets whose refractive index does not much any more with that of the polymeric matrix. As a consequence, the light transmission becomes lower. Heating is produced also by the pump beam partially absorbed by the sample. As a matter of fact, the contrast between the two stats is limited byt the fact that it is difficult to have a sample where the isotropic refractive index of the liquid crystal is very different from that of the polymer. In addition, a different behavior for different polarization of the probe beam with respect to the pump one was found, which is an index of the presence of a light field induced reorientation.

Other geometrical configuration which can lead to self-transparency or self-limiting effects are those involving stretched structures of PDLC. For example, the self-limiting effect described above may be

enhanced stretching the sample during the curing process in order to obtain elliptical droplets. In this way the sample transmission becomes more sensitive to the light polarization and, when the pump intensity is increased, isotropization of the droplets may change the index mismatch more efficiently.

5.3. Nonlinear Gratings and Threshold Degenerate Wave Mixing

The switching behavior associated to self-transparency affects the wave mixing phenomenon in peculiar way. Degenerate wave mixing has been extensively studied in the part few years in the wide range of materials [37]. It is well known that when two laser beams of the same wavelength cross each other at a small angle in a nonlinear material they can interact through the nonlinear polarization of the medium with the result that new coherent waves at the same wavelength are generated, travelling in different directions. These new waves can be considered the result of the diffraction of the impinging beams by the grating produced by their interference in the nonlinear material. In liquid crystals, this interference pattern gives rise to an index modulation which in turn produces a phase grating. The light intensity on the sample can therefore be written as

$$I = I_0[1 + m\cos(2\pi x/\Lambda)] \tag{114}$$

where $I_0 = I_1 + I_2$ is the sum of the intensities of the two impinging beams, x is the transversal coordinate, Λ is the grating constant related to the vacuum wavelength λ_0, the refractive index n of the medium and the crossing angle θ by the equation $\Lambda = \lambda_0/(n\sin\theta)$. and finally m is the linear modulation index (also called fringes contrast) defined as $m = 2(I_1 I_2)^{1/2}/(I_1 + I_2)$.

In PDLC a strong nonlinear response has been found due to thermal effects, therefore, we will focus the following discussion on thermal gratings owing to the modulation of the refractive index induced by a periodic variation of the temperature distribution. Some studies have been performed on the formation of nonlinear gratings induced by thermooptical-optical effects in PDLC [38]. Experiments have been carried out on dye-doped samples using the standard configuration shown in Figure 22, either in the low modulation ($m \ll 1$) or under the maximum contrast ($m \approx 1$) condition.

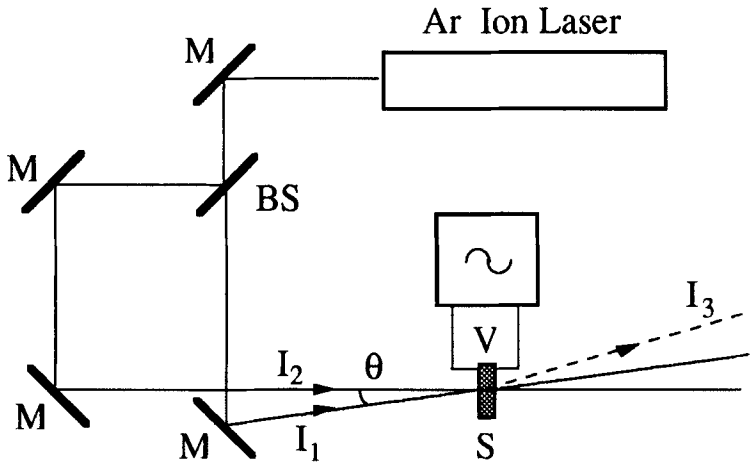

FIGURE 22 Experimental set-up used to study nonlinear diffraction induced by thermooptical-optical effects in PDLC.

A very peculiar feature of these thermal gratings in PDLC is the occurrence of a threshold effect associated to the self-transparency. When two laser beams interact in a PDLC, no transmission occurs as far as the light intensity I_0 is lower than the threshold value I_0th which is necessary to induce self-transparency. In the low modulation condition (*i.e.*, $I_1 \gg I_2$) one has $I_0 \approx I_1$ and thus it is the pump beam which determines the onset of transparency, controlling both its own transmission and the transmission of the probe (signal) beam. This effect realizes an opto-optical switch. The sharp switching of the signal driven by the pump beam is evident in Figure 23, where the transmitted probe signal is drawn against I_1. A similar power-dependent transmission behavior is induced on the transmitted pump beam itself. Of course, in the high modulation condition $m \approx 1$ ($I_1 \approx I_2$) both beams are effective for reaching the self-transparency threshold.

When self transparency is established ($I_0 > I_0^{\text{th}}$), if the coherence conditions are fulfilled [14], diffracted beams appear after the sample due to the wave mixing. The situation is in general very complex but the description of the peculiar features of the effect greatly simplifies when only the brightest diffracted beam (*i.e.*, the first diffracted beam) characterized by the wavevector k_3 is considered (see Fig. 24). Using

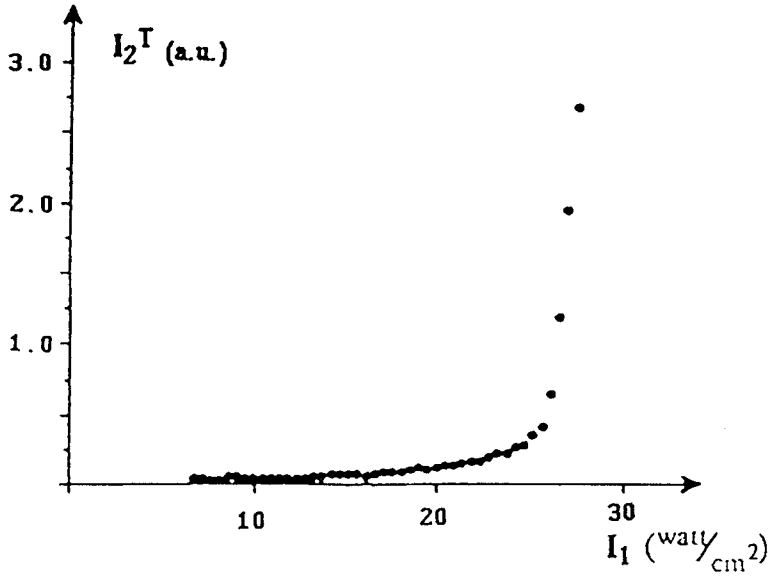

FIGURE 23 Transmitted signal I_2^T *vs.* pump intensity I_1 (after Ref. [35]).

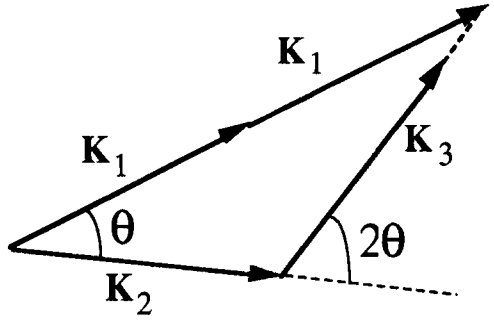

FIGURE 24 Diagram of the wavevectors in the wave-mixing process. $\mathbf{K}_1$ and $\mathbf{K}_2$ are the wavevectors of the pump and probe (signal) beam, respectively. $\mathbf{K}_3 = 2\mathbf{K}_1 - \mathbf{K}_2$ is the wavevector of the first diffracted beam. An efficient generation of the first diffracted beam requires a small value of the phase mismatch $\Delta\mathbf{k} = 2\mathbf{K}_1 - \mathbf{K}_2 - \mathbf{K}_3$, *i.e.*, a small values of the crossing angle θ.

standard calculation [14], it can be shown that the intensity of the first diffracted beam in the low modulation approximation is given by

$$I_3 = \beta I_1^2 I_2 \tag{115}$$

where I_1 and I_2 are the intensities of the incoming beams and the constant β includes the square of the index gradient $(dn/dT)^2$.

When $(I_0 > I_0^{th})$, isotropic droplets develop in the area crossed by the beams and the refractive index in this area is modulated by the fringes distribution. The grating characteristics of PDLC were studied by measuring either I_3 *vs.* I_2 (with I_1 constant) and I_3 *vs.* I_1 (with I_2 constant) and the dependence expressed by Eq. (115) has always been found (see Fig. 25). In Figure 25 there is also well evident the threshold behavior of the nonlinear diffraction, which is the most important and peculiar feature of self-diffraction in PDLC. The measured time decay of the gratings agree with the isotopic thermal diffusivity values of nematic LCs.

The threshold value I_0^{th} depends on the scattering properties of the sample, because the scattering affects the penetration depth of the radiation into the sample and the consequent heating. In fact, an optimum value of the scattering exists which maximizes absorption. As in PDLC the amount of light scattering is easily controlled by the application of a low frequency voltage, it is possible in these samples to

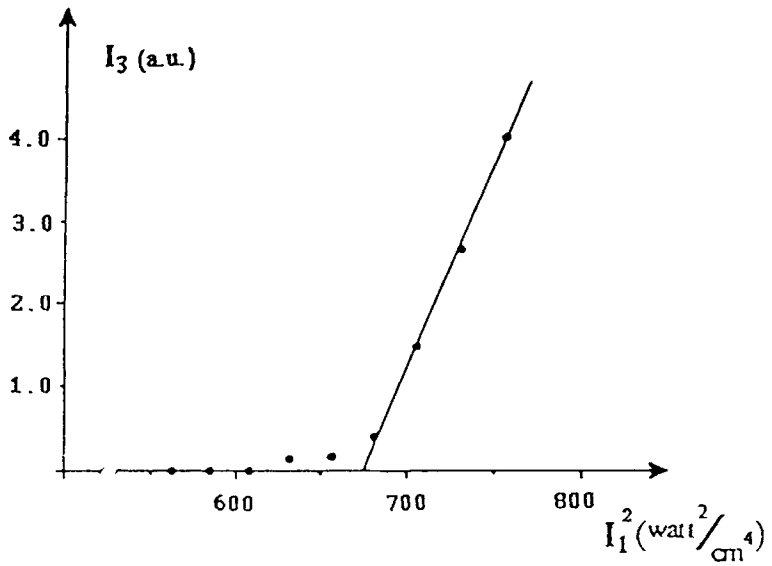

FIGURE 25 Intensity of the brightest diffracted beam I_3 *vs.* I_1^2 (after Ref. [35]).

control the value I_0^{th} and, most important, to drive the nonlinear diffraction by the applied voltage. To this purpose, it is sufficient to set the intensity I_0 to a value $I_0 > I_0^{th}$ such that transmission is inhibited when the applied voltage V is zero whereas self-diffraction occurs when the voltage is switched on. Figure 26 reports the result of an experiment where the intensity of the diffracted beam *vs.* time was measured under a low frequency (10 Hz) square voltage applied to the sample.

By increasing the amplitude of the applied voltage, the light transmission through the sample increases with consequent absorption and formation of the grating, thus leading to diffracted beams whose intensity is dependent on the applied voltage.

Another interesting effect is observed in the dual experiment where the intensity I_0 is varied while the amplitude of the applied square

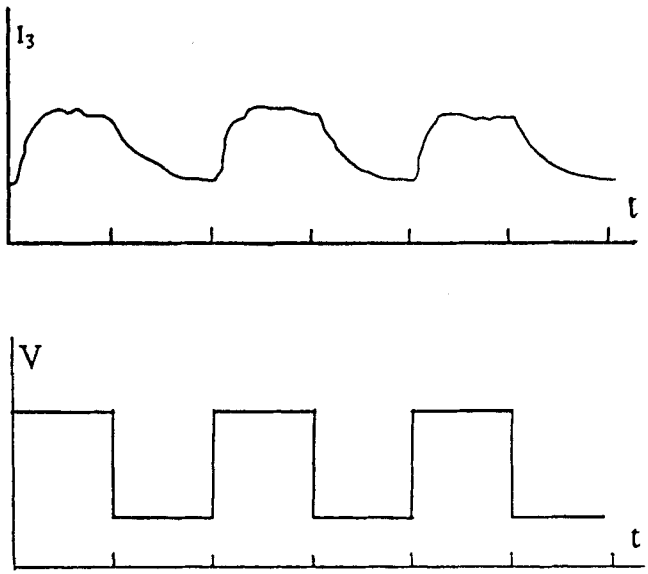

FIGURE 26 (a) Intensity of the first diffracted beam I_3 *vs.* time. (b) Applied square voltage *vs.* time (oscilloscope traces). $I_0 = 25\,W/cm^2$, $V = 30\,V$, time scale 50 ms/div. The data show how it is possible to drive the intensity of the diffracted beam by the applied voltage. The experiment was performed in the usual configuration for degenerate wave mixing fixing the total laser power in order to have $I_0 = I_1 + I_2 < I_0^{th}$. Observations were made on a sample characterized by a switch-on voltage of about 50 V (after Ref. [35]).

wave voltage is kept at a constant value. A typical example of the shape of the diffracted signal in the time domain is shown in Figure 27.

The two peaks following the switch-on and switch-off of the voltage can be explained by assuming the onset of a *transient amplitude grating* in the sample [35, 38]. This effect is possible in general when the switch-on time τ_{on} depends on the light intensity [39] and this is the case in PDLC. In fact, τ_{on} is a function of the applied voltage and, since the switch-on voltage depends on the temperature, we have a local temperature rise due to light absorption in the sample so that $\tau_{on} = \tau_{on}(I)$. As a consequence we expect that, when a voltage is applied to the sample to switch it to the transparent state, the risetime τ_{on}^{M} in the regions of the sample corresponding to the maxima of the thermal grating will be shorter that the one, τ_{on}^{m}, in the regions of the minima. Then, in the time interval between τ_{on}^{M} and τ_{on}^{m} transmission channels settle up in the location of the maxima thus getting a transient amplitude grating. Differently from the phase gratings which are characterized by modulation of the refractive index, in the amplitude grating one has modulation of the transmission in a plane transversal to the propagation direction. After the time τ_{on}^{M} a uniform transmission is reached on the laser spot (since it does not depend on

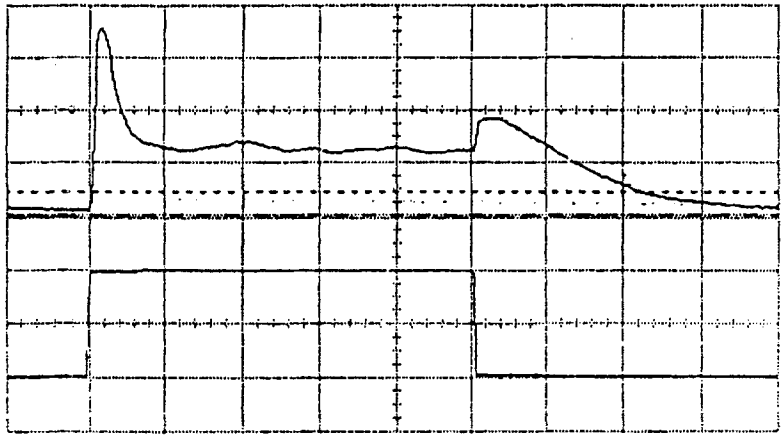

FIGURE 27 Hard copy of the oscilloscope trace. Channel 1: diffracted intensity; channel 2: applied voltage. Time scale: 10 ms/div (after Ref. [35]).

the intensity) whereas only a phase grating is possible in the steady state (for times longer than τ_{on}^{m}). A similar behavior is expected when the voltage is switched off, however, a much weaker effect is usually observed because of the very weak dependence of τ_{off} on the intensity [35].

In principle, it seems to be possible to create a steady amplitude grating in PDLC. In fact, if the total intensity I_0 on the sample and the index modulation m are adjusted such that $I_m = I_0(1-m) < I_{th}$ and $I_M = I_0(1+m) > I_{th}$, where I_m and I_M are the minimum and maximum intensity of the fringes pattern, respectively, self-transparency should occur only at the location of the intensity maxima, thus producing a transmission grating. However, no experimental verification of this effect has been reported up to now. On the contrary recently the formation of permanent gratings in PDLC has been reported [40]. By using an holographic arrangement in the phase of photopolymerization of PDLC compounds a novel system with periodic planes of droplets has been obtained. It has been demonstrated that these gratings are electrically switchable and a good control of the diffraction efficiency can be achieved.

An orignal application of self-diffraction to measure the duration of short pulses has recently been reported [41]. This technique exploits the diffraction from a transient grating obtained by the beam-splitting of the measured pulse and the introduction of a variable delay line between the two interfering beams. The experimental set-up is shown in Figure 28.

The intensity of the diffracted beam is measured versus the delay time τ_d and a typical example of the results obtained with this technique is shown in Figure 29.

The pulse duration τ_p is simply calculated from the measurement of the full width at half maximum Δ of the Gaussian function describing the diffracted intensity *vs* τ_d, by means of the equation

$$\tau_p = \frac{\Delta}{\sqrt{2}} \tag{116}$$

In fact, when the source beam is splitted and the two secondary beams superimpose to create the dynamical grating, the diffraction efficiency is related to a product of four radiation fields. More precisely, it

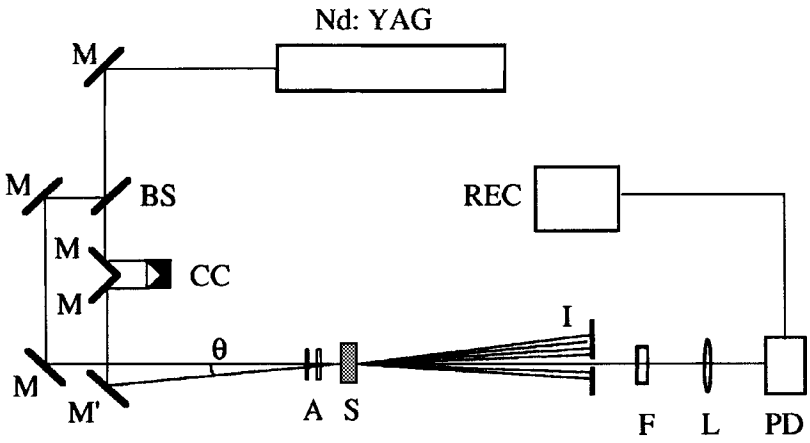

FIGURE 28 Experimental set-up used to perform measurements of the duration of short pulses. The source of short pulses is a linearly polarized second harmonic beam ($\lambda = 532$ nm) obtained by a continuously mode-locked N_d-YAG laser at a repetition rate of 76 MHz. The beam is split in a Mach-Zender type interferometer where a delay line is introduced in one harm. The two outcoming beams cross each other at a small angle on the PDLC sample to create a thermal grating (after Ref. [41]).

becomes proportional to the integral function $\eta(t)$ given by [41]

$$\eta(t) = \frac{1}{\tau_p^2} \int_{-\infty}^{t} C(t_1)C(t_1 + \tau_d)C(t_2)C(t_2 + \tau_d)f(u)dt_1 dt_2 \qquad (117)$$

where τ_d indicates the time delay between the two pulses and

$$f(u) = \langle u(L_1)u(L_2 + \tau_d)u^*(t_2)u^*(t_1 + \tau_d)\rangle \qquad (118)$$

is the expectation value of the product of four fields. In Eqs. (117) and (118) the functions $C(t)$ are given by

$$C(t) = e^{-2\ln(2t^2/\tau_p^2)} \qquad (119)$$

and $u(t)$ represent the amplitude shape factor and the phase factor, respectively, of the time dependent part of the electric field of the pulse $E(t)$ written as $E(t) = EC(t)u(t)$. In the limit of very long relaxation times of the material, $t \to \infty$ and $f(u)$ becomes simply the fourth order coherence function of the field. Then, the function $\eta(t)$ reduces to

$$\eta(t) = e^{-2\ln(2\tau_d^2/\tau_p^2)} \qquad (120)$$

from which Eq. (116) is easily obtained.

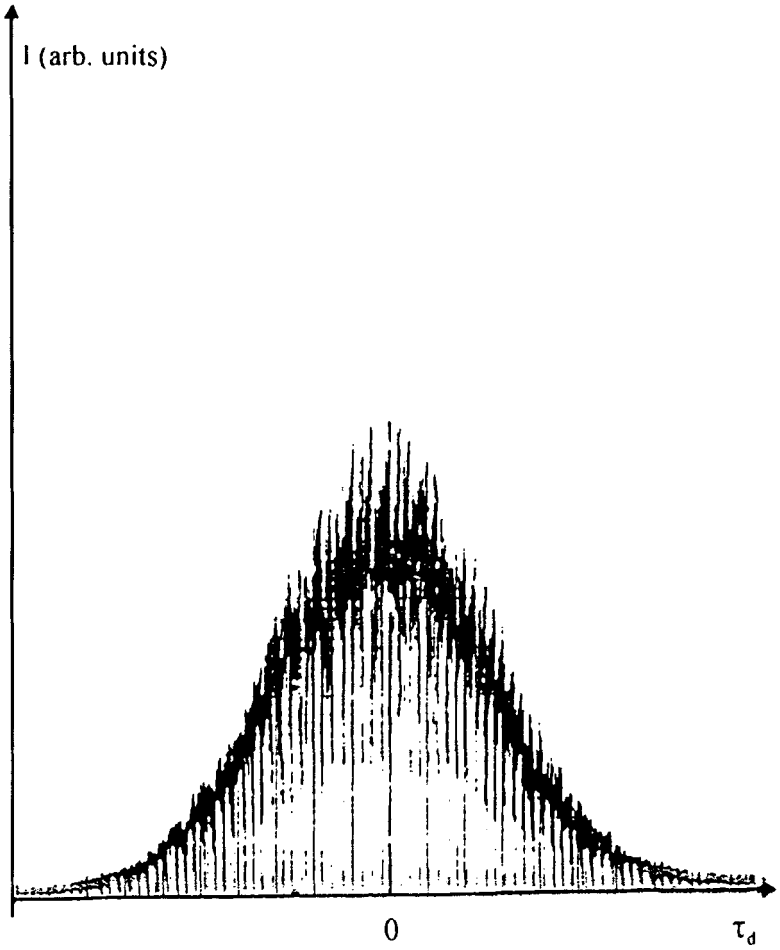

FIGURE 29 Typical shape of the intensity of the first diffracted beam as function of the delay time τ_d. In the experiment described in Ref. [41] the pulse width calculated from the full width at half maximum of the curve according to Eq. (124) is $\tau_p = 46.9 \pm 2.2$ ps which is in very good agreement with the value 46.7 ± 1.5 ps obtained by the conventional second harmonic generation autocorrelation technique.

5.4. Optical Bistability

Bistability is in general an effect which involves the occurrence of a hystheresis in the output-input characteristic of a given device. The presence of hystheresis in the transmission characteristic of PDLC has

been reported both in the case of temperature [16] and voltage [33] as variable parameter.

Optical bistability, where hystheresis is controlled by the intensity of the impinging light, is a very interesting effect for the application of PDLC as optical storage devices. As first pointed out by D.A.B. Miller [42], a physical system where the light absorption increases with the impinging light intensity may exhibit an optical bistable behavior; in this case it is just the effect of light-induced increasing absorption which operates as intrinsic feedback mechanism. Such a situation has been recently obtained with dye doped PDLC samples [43]. The highly dichroic dye was used both to increase the light absorption and to obtain different absorptions for different director orientations in the nematic droplets. Here the molecules have an average alignment parallel to the liquid crystal director **n** and, therefore, if the director orientation changes, a strong dichroic effect must be expected according to the ratio $\alpha = A_{\parallel}/A_{\perp}$, where $A_{\parallel}$ and $A_{\perp}$ are the absorption coefficients parallel and perpendicular to the molecular axis, respectively. If we suppose the droplets completely aligned by a static electric field and the light travelling in the sample at normal incidence (*i.e.*, the polarization is perpendicular to the applied field), the absorption A_1 in the low optical power region can be written as

$$A_1 = s' A_{\perp} + (1 - s')\left(\frac{2A_{\perp} + A_{\parallel}}{3}\right) \tag{121}$$

where s' is the order parameter of the dye molecules. The factors s' and $(1-s')$ in Eq. (121) weight the anisotropic contribution due to the ordered molecules and the isotropic contribution due to the disordered molecules, respectively. When, increasing the light intensity, the droplets become isotropic, the high optical power regime is reached, where the total absorption A_2 equals the isotropic absorption A_{iso}

$$A_2 = A_{\text{iso}} = \frac{2A_{\perp} + A_{\parallel}}{3} \tag{122}$$

For strongly dichroic dye molecules it is $A_{\parallel} \gg A_{\perp}$ and then $A_2 \gg A_1$ which leads to optical bistability. In fact, assuming the temperature rise proportional to the impinging power through the absorption A_s

$$\Delta T = cAP_i \tag{123}$$

(c is a constant) we can write toa first approximation (step-like model)

$$A_s(\Delta T) = \begin{cases} A_1 & \text{for } \Delta T < T_c - T_0 \\ A_2 & \text{for } \Delta T > T_c - T_0 \end{cases} \tag{124}$$

where T_c is the transition temperature to the isotropic state and T_0 is the room temperature. The transmission t of the sample can be written as

$$t = \kappa(1 - A_s) = \kappa\left(1 - \frac{\Delta T}{\eta P_i}\right) \tag{125}$$

where κ is a constant allowing for all non absorptive losses. The bistable behavior of the device becomes immediately evident when a graphical solution of the system of Eqs. (123) and (124) is considered, as shown in Figure 30.

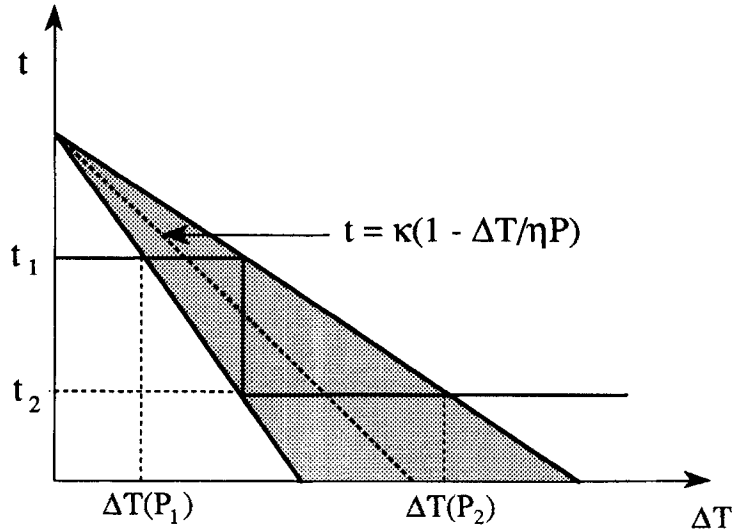

FIGURE 30 Transmission t *vs.* the temperature rise ΔT for the device operating according to the step-like model described by Eqs. (123) and (124). The straight lines are the plots of Eq. (125) for three different values of the impinging power. P_1 and P_2 ($P_1 < P_2$) are the critical values of the input power which cause switching between the two transmission states. Increasing P_i starting from $P_i < P_1$, transmission keeps the initial value $t_1 = \kappa(1 - A_1)$ until P_i reaches the value P_2 where t jumps abruptly to the lower value $t_2 = \kappa(1 - A_2)$. Once reached this condition, a reduction of P_i does not change the transmission until the power P_1 is reached where a transmission jump to the higher value t_1 takes place.

In the region $P_1 < P < P_2$ we have three solutions for the transmission $t(\Delta T)$, that it, three values for the output power $P_0 = tP_i$. Therefore, this is an optical bistability region whose width, W defined as $W = (P_1 - P_2)/P_1$, is given by (see Eq. (123))

$$W = (P_2 - P_1)/P_1 = 1 - A_1/A_2 \tag{126}$$

The last equation shows that is possible to obtain a large bistability loop ($W \to 1$) by a proper choice of the dye molecules.

The simple model discussed here provides a qualitative description of the bistability effects experimentally observed in PDLC. A more detailed description needs the consideration of the beam shape effects and the temperature dependence through the phase transition of the parameter κ. Figure 31 shows the experimental set-up used in the experiments.

In Figure 31 the measured transmitted signal *vs.* the impinging power is reported for different values of the applied voltage. This behavior is in good qualitative agreement with the model presented. The bistable behavior becomes more and more evident as the applied voltage increases. The slope of each curve (which is proportional to the light transmittivity) decreases from the low to the high optical power regions and the slope in the high optical power region is the same for each curve. Thus the ratio of the high transmittivity T_2 to the low

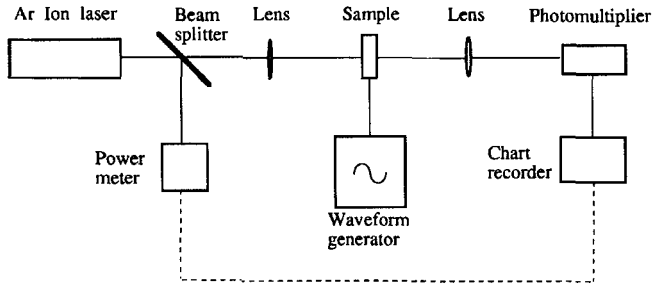

FIGURE 31 Sketch of the experimental set-up used to perform measurements of optical bistability in dye doped PDLC. The light beam from an Argon Ion laser (λ = 5145 Å) is linearly polarized and focused (f = 100 mm) on the dye doped PDLC sample at normal incidence; the transmitted optical power is detected by a photomultiplier and sent to a chart recorder. A beam splitter placed before the sample allows to measure the impinging light power P_i. An ac (10 KHz) voltage is applied to the conducting glasses to switch the sample to the low scattering state. The dye used gives a ratio $\alpha = A_{\parallel}/A_{\perp} = 10$ and makes it possible to get on order parameter $S' \approx 0.6$.

transmittivity T_1 increases with the applied voltage and, as expected, the same occurs for the width of the bistability loop.

A different experimental scheme, *i.e.*, a classical hybrid configuration, was used by Kim and Palffy-Muhoray [44] to obtain optical bistalbe behavior (see Fig. 32).

In this configuration, the voltage across the sample cell is a linear function of the transmitted power P_0

$$V_c = V_0 + \mathrm{GP}_0 \tag{127}$$

where V_0 is the offset voltage and G the gain of the feedback circuit. By writing $P_0 = tP_i$ we easily get

$$t = (V_c - V_0)/\mathrm{GP}_i \tag{128}$$

In the case of negative feedback ($G < 0$) one gets a power limiting behavior. Differently, a positive feedback ($G > 0$) gives rise to optical bistability as shown by Figure 33 where Eq. (128) is plotted (dashed straight line) together with the characteristic $t(V_c)$ of the PDLC sample (solid line). The range of P_i values which corresponds to three intersection between the two curves correspond to the bistable region.

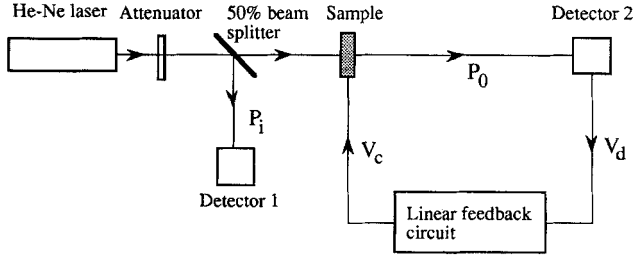

FIGURE 32 Hybrid configuration for the study of optical bistability in PDLC. The sample is illuminated by an attenuated He-Ne laser beam and the transmitted intensity is detected by a photodiode. The feedback circuit provides a voltage which is a linear function of the photodiode amplifier output. This voltage is used to modulate the output of a waveform generator driving the voltage applied to the sample.

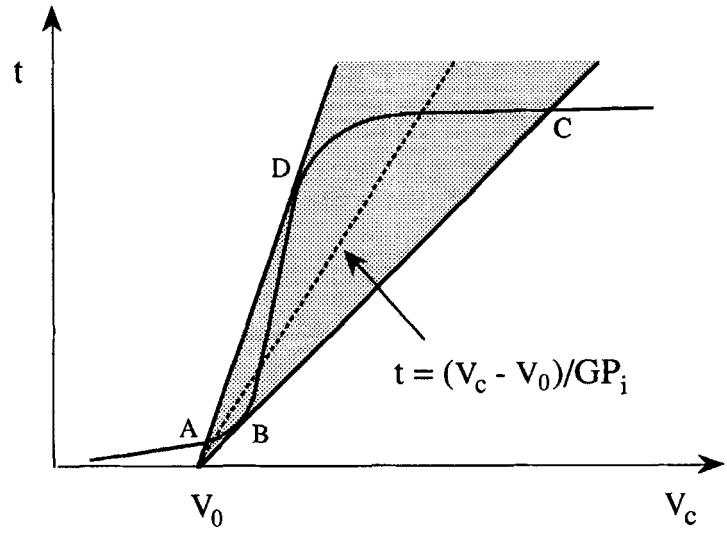

FIGURE 33 Transmission t *vs.* the feedback voltage V_c for the device operating according to hybrid configuration of Figure 32. The curved full line represents the transmission characteristic $t(V_c)$ of the PDLC sample whereas the straight lines are the plots of Eq. (126) for three different values of the impinging power P_i. The range where there are three intersections corresponds to the bistable region: by increasing P_i the slope of the straight line becomes lower and lower and the operating point is in the branch between A and B. A further increase of the incident power causes a jump to the upper part of the curve and the operating point becomes C. If we now decrease the power, the branch from C to D is stable and the system keeps the high transmission state until the point D is reached where a jump to the low branch occurs. Accordingly, we have a bistable loop between the critical points B and D.

5.5. Second Harmonic Generation

Second Harmonic generation (SHG) is a typical and well known nonlinear optical effect which occurs in non-centrosymmetric materials where the second order susceptibility $\chi^{(2)}$ is different from zero. When a light wave with frequency ω propagates in these materials, a nonlinear polarization

$$\mathbf{P}(2\omega) = \underline{\chi}^{(2)} : \mathbf{E}(\omega)\mathbf{E}(\omega) \tag{129}$$

is induced which acts as a source term in the Maxwell's equations and generates a second wave having a double frequency 2ω.

Nematic liquid crystals, as well as most of the polymers used in the preparation of PDLC, have usually a centre of symmetry on a macroscopic scale. Therefore, SHG is in principle forbidden for these materials. Nevertheless, a Second Harmonic signal in PDLC is expected, and actually has been observed [45, 46], due to the huge number of interfaces which are present. In fact, at the interfaces the symmetry is broken and SHG becomes no more forbidden. This effect is called Surface Induced Second Harmonic Generation (SISHG). Symmetry can be broken also by the application of an external dc electric field to the sample; in this case we speak of Electrical Field Induced Second Harmonic Generation (EFISHG).

In the recent years, the effect of SISHG has been systematically studied and applied to many different materials. The origin of the surface nonlinear susceptibility has been explained by Shen [47]. In this model, the interface is considered as a polarization sheet with dielectric permittivity ε' and surface polarization $\mathbf{P}^s$

$$\mathbf{P}^s(2\omega) = \underline{\chi}_s^{(2)} : \mathbf{E}_L(\omega)\mathbf{E}_L(\omega) \tag{130}$$

where $\mathbf{E}_L(\omega)$ is the local field related to the incoming field by the Fresnel coefficients and $\chi_x^{(2)}$ is the second order surface susceptibility. If the interfacial plane layer I is normal to the z axis and has a finite thickness, with plane boundaries located at $z = 0^-$ and $z = 0^+$, the terms of $\underline{\chi}_s^{(2)}$ take the following form

$$\begin{aligned}\chi_{s,ijk}^{(2)} = \eta_i(2\omega) \int_I \Big[& \chi_{ijk}^D s_i(2\omega) s_j(\omega) s_k(\omega) \\ & + \chi_{izjk}^Q s_j(\omega) s_k(\omega) \frac{\partial}{\partial z} s_i(2\omega) \Big] dz \\ + \eta_i(2\omega) \Big\{ & \left[\chi_{izjk}^Q s_i(2\omega) s_j(2\omega) s_k(\omega) \right]_{z=0^-} \\ & - \left[\chi_{izjk}^Q s_i(2\omega) s_j(2\omega) s_k(\omega) \right]_{z=0^+} \Big\}\end{aligned} \tag{131}$$

where $\eta_i = s_i = 1$ for $i = x, y$, $\eta_z = \varepsilon$' and $s_Z(z) = Ez(z)/Dz(z)$. In the last equation different contributions are recognized. The quantity under the sign of integral depends on the properties of the interface: in particular, the first term is an electric dipole contribution originated by the symmetry break at the boundary surface and the second one is

a quadrupolar contribution which is associated to the rapid field variation across the interface. The term outside the integral originates from the structural difference of the media and depends only on bulk material parameters. For isotropic materials, this analysis gives the following equations for the non vanishing surface susceptibility terms of the third order tensor $\underline{\chi}_s^{(2)}$

$$\begin{aligned}
\chi_{zzz} &= \chi_{S'zzz} - \frac{\gamma + \chi_1^Q}{\varepsilon(2\omega)\varepsilon(\omega)^2} \\
\chi_{zyy} &= \chi_{zxx} = \chi_{S'zxx} - \frac{\gamma + \chi_2^Q}{\varepsilon(2\omega)} \\
\chi_{yzy} &= \chi_{xzx} = \chi_{S'xzx} - \frac{\chi_4^Q}{\varepsilon(\omega)}
\end{aligned} \tag{132}$$

where $\chi_1^Q = \chi_{iiii}^Q$, $\chi_2^Q = \chi_{iijj}^Q$, $\chi_4^Q = \chi_{ijji}^Q$ and the surface contribution $\chi S'_{iii}$ is separated from the actual bulk contribution (represented by γ). and the contribution χ^D due to the field gradient at the interface. For liquid crystal molecules one can usually assume $\gamma = 0$.

On the basis of the above results, in PDLC each droplet can be considered as a source of a second harmonic signal due to both the contribution of the polymer-liquid crystal interface (which is affected by the particular molecular order on the surface) and the contribution of the permittivity mismatch (which gives rise to a field gradient across the droplet boundaries). However, a complete understanding of the nature of SHG in PDLC deserves still further detailed investigations. The real contribution of electric-dipole origin in the spherical cavity seems to be questionable. Moreover, since the application of an external voltage changes the mismatch between the two media, the SHG due to the field gradient should be sensitive to the applied voltage. An additional contribution to SHG originating from the bulk of the droplet could be associated to possible high distortions of the director orientation inside the droplets which cause a lost of symmetry of the nematic liquid crystal thus originating a second order susceptibility of electric-dipole nature.

As reported by Pallfy-Muhoray and coworkers [45] SHG may represent a useful tool to monitor the phase separation process of the droplets in the preparation of PDLC by the PIPS method. This is one

possible application of SHG but the arguments and observation reported in this brief discussion of the phenomena suggests that SHG in PDLC is potentially a very promising method of investigation.

References

[1] Crawford, G. P. and Doane, J. W. (1992). *Condensed Matter News*, **1**, 5.
[2] Doane, J. W., Chidichimo, G. and Vaz, N. A. (1987). U.S. Patent, N. 4688900.
[3] Drzaic, P. S. (1986). *Jour. Appl. Phys.*, **60**, 2142; Vaz, N. A., Smith, G. W. and Montgomery, G. P. Jr. (1987). *Mol. Cryst. Liq. Cryst.*, **146**, 1 and (1987). *Mol. Cryst. Liq. Cryst.*, **146**, 17 (1987); Westk, J. L. (1988). *Mol. Cryst. Liq. Cryst.*, **157**, 427.
[4] Frank, F. C. (1958). *Discu. Faraday Soc.*, **25**, 19.
[5] Ames, W. F. (1977). Numerical Methods for Partial Differential Equations. (Academic, New York).
[6] Volovik, G. E. and Larentovich, O. D. (1983). *Sov. Phys. JETP*, **58**, 1159; Ondris-Crawford, R., Boyko, E. P., Wagner, B. G., Erdmann, J. H., Zumer, S. and Doane, J. W. (1991). *J. Appl. Phys.*, **69**, 6380.
[7] Drzaic, P. S. (1988). *Mol. Cryst. Liq. Cryst.*, **154**, 289.
[8] Erdmann, J. H., Zumer, S. and Doane, J. W. (1990). *Phys. Rev. Lett.*, **64**, 1907.
[9] Jackson, J. D. (1985). *Classical Electrodynamics* (John Wiley, New York).
[10] Kelly, J. R. and Palffy-Muhoray, P. (1991). *ALCOM Series*, **1**, 1 and Kelly, J. R. and Palffy-Muhoray, P. (1994). *Mol. Cryst. Liq. Cryst.*, **243**, 11.
[11] Palffy-Muhoray, P. (1989). *SPIE Proc.*, **32**, 1080.
[12] Frank, F. C. (1958). *Disc. Faraday Soc.*, **25**, 19.
[13] Kelly, J. R. and Seekola, D. (1990). *SPIE Proc.*, **1257**, 17.
[14] Simoni, F. (1996). *Nonlinear Optical Properties of Liquid Crystals and Polymer Dispersed Liquid Crystals* (World Scientific Publishing Co., Singapore).
[15] Doane, J. W., Vaz, N. A., Wu, B. G. and Zumer, S. (1986). *Appl. Phys. Lett.*, **48**, 269; Wu, B. G., Erdmann, J. H. and Doane, J. W. (1989). *Liquid Crystals*, **5**, 1453.
[16] Drzaic, P. S. (1988). *Liq. Crystals*, **3**, 1543.
[17] Zumer, S., Golemme, A. and Doane, J. W. (1989). *J. Opt. Soc. Am.*, **6**, 403.
[18] Zumer, S. (1988). *Phys. Rev.*, **A37**, 4006.
[19] Zumer, S. and Doane, J. W. (1986). *Phys. Rev.*, **A34**, 3373.
[20] Keller, H. and Hatz, R. (1980). Handbook of Liquid Crystals (Verlag Chemie, Weonheim).
[21] Lord Rayleigh (1871). *Philos. Mag.*, **41**, 107; **41**, 274 (1871); **41**, 447 (1871).
[22] Gans, R. (1925). *Ann. Phys.*, **76**, 29.
[23] Basile, F., Bloisi, F., Vicari, L. and Simoni, F. (1993). *Phys. Rev.*, **E48**, 432.
[24] Fuh, A. Y. G., Ko, T. C., Chyr, Y. N., Huang, C. Y., Tzen, B. W. and Sheu, C. R. (1993). *Japan. Jour. Appl. Phys.*, **32**, 3526.
[25] Basile, F., Bloisi, F., Vicari, L. and Simoni, F. (1994). *Mol. Cryst. Liq. Cryst.*, **251**, 271.
[26] Simoni, F., Bloisi, F. and Vicari, L. (1992). *Mol. Cryst. Liq. Cryst.*, **223**, 169.
[27] Bloembergen, N. (1965). Nonlinear Optics (Benjamin, New York).
[28] Yariv, A. (1975). Quantum Electronics, II edn. (Wiley, New York).
[29] Zel'dovich, B. Ya., Pilipetskii, N. F., Sukhov, A. V., Tabiryan, N. V. (1980). *JETP Lett.*, **31**, 264.
[30] Tabiryan, N. V., Sukhov, A. V., Ya Zeldovich, B. (1986). The Orientational Optical Nonlinearity of Liquid Crystals; *Mol. Cryst. Liq. Cryst.*, **136**, 140 and the references therein.

[31] Khoo, I. C. (1988). Nonlinear Optics of liquid Crystals, *Prog. Optics.*, **27**, 107 and references therein.
[32] Simoni, F., Cipparrone, G., Umeton, C., Arabia, G. and Chidichimo, G. (1989). *Appl. Phys. Lett.*, **54**, 896 (1990); *Mol. Cryst. Liq. Cryst.*, **179**, 269.
[33] Palfy-Muhoray, P. and West, J. L. (1988). *SPIE*, **927**, 226; Palfy-Muhoray, P. (1989). *SPIE*, **1080**, 91 (1989); Palfy-Muhoray, P., Frisken, B. J., Kelly, J. and Yuan, H. J. (1989). *SPIE*, **1105**, 33.
[34] Al'tshuler, G. B. and Ermolaev, V. S. (1983). *Sov. Phys. Dokl.*, **28**, 146; Al'tshuler, G. B., Ermolaev, V. S., Krylov, K. I. and Manenkov, A. A. (1983). *Sov. Phys. Dokl.*, **28**, 951.
[35] Simoni, F., Bloisi, F. and Vicari, L. (1993). *Int. J. Nonlinear Opt. Phys.*, **2**, 353.
[36] Pallfy-Muhoray, P., Lee, M. A. and West, J. L. (1990). *Mol. Cryst. Liq. Cryst.*, **179**, 445.
[37] Fisher, R. (1984). Optical Phase Conjugation (Academic, New York; Khoo, I. C. Progress in Optics, Wolf, E. Ed. (1988). (North Holland, Amsterdam), Vol. XXVI.
[38] Simoni, F., Cipparrone, G., Duca, D. and Khoo, I. C. (1991). *Opt. Lett.*, **16**, 360; Simoni, F., Bloisi, F., Duca, D. and Vicari, L. (1992). *Mol. Cryst. Liq. Cryst.*, **212**, 279; Simoni, F., Bloisi, F. and Vicari, L. (1992). *Mol. Cryst. Liq. Cryst.*, **223**, 169.
[39] Goodman, J. W. (1968). Introduction to Fourier Optics, (Mc Graw Hill, N.Y.).
[40] Sutherland, R. L., Tondiglia, V. P., Natarajan, L. V., Bunning, T. J. and Adams, W. W. (1994). *Appl. Phys. Lett.*, **64**, 1074.
[41] Cipparrone, G., Duca, D., Mazzulla, A., Umeton, C. and Simoni, F. (1993). *Optics Comm.*, **97**, 54.
[42] Miller, D. A. B. (1984). *J. Opt. Soc. Am.*, **18**, 857.
[43] Simoni, F., Cipparrone, G. and Umeton, C. (1990). *Appl. Phys. Lett.*, **57**, 1949 (1991); Simoni, F., Cipparrone, G. and Umeton, C. (1991). *Mol. Cryst. Liq. Cryst.*, **207**, 231.
[44] Kim, J. Y. and Palffy-Muhoray, P. (1989). *Jour. Appl. Phys.*, **66**, 362.
[45] Li, L. and Yuan, H. J. and Palffy-Muhoray, P. (1991). *Mol. Cryst. Liq. Cryst.*, **198**, 239; (1991) and *SPIE*, **1455**, 73.
[46] Vogeler, T., Kreuzer, M. and Simoni, F., *Proceedings of VI Inter. Top. Meeting on Optics of Liquid Crystals, OLC'95*, in press on *Mol. Cryst. Liq. Cryst.*
[47] Guyot-Sionnest, P., Chen, W. and Shen, Y. R. (1986). *Phys. Rev.*, **B33**, 8254; Guyot-Sionnest, P. and Shen, Y. R. (1988). *Phys. Rev.*, **B38**, 7985; Shen, Y. R. (1988). *Nature*, **337**, 519; (1989) and *Ann. Rev. Phys. Chem.*, **40**, 327.